Self-Assembled Monolayers and Multilayers

Structures and Applications

Yu-Tai Tao

Outline

- Basic Structures
  - Langmuir Monolayers
  - Self-Assembled Monolayers (SAMS)
    - → Carboxylic acids on oxide surfaces
    - → Alkylsilanes on hydroxylated surfaces
    - → Organothiol on coinage metals
  - Mixed monolayers
  - Mutilayers
  - Monolayer-protected clusters(MPCs)
- Applications of SAMs
  - Soft lithography
  - Nonlinear Optical (NLO) materials
  - Molecular electronics

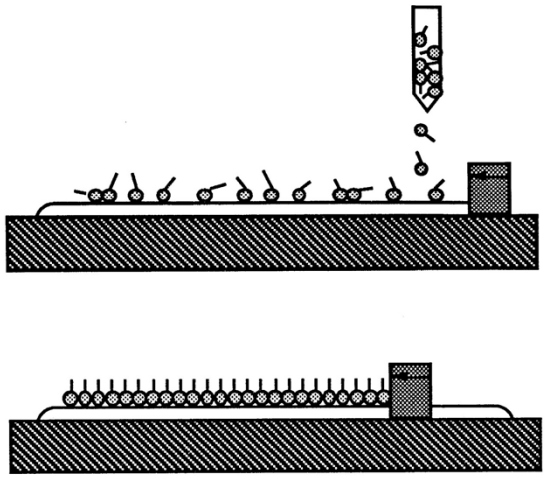

Figure 1. A monolayer of molecules in a two-dimensional gas (top), and in the compressed form (bottom).

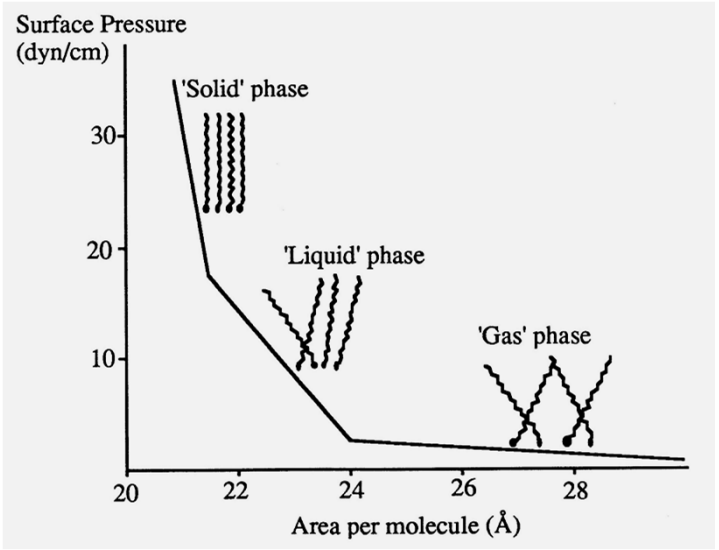

Figure 2. A scheme of surface pressure (π) vs. area per molecule (Å) for stearic acid on 0.01M HCl.

Langmuir-Blodgett Films

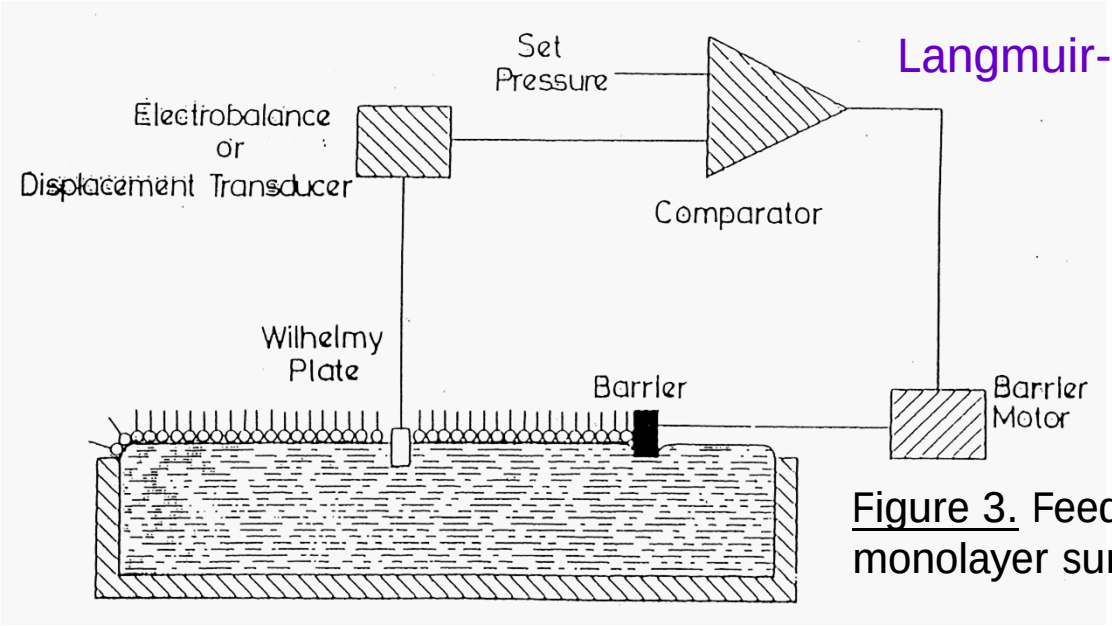

Figure 3. Feedback loop to control monolayer surface pressure.

Amphiphiles: A molecule that is insoluble in water, with one end that is hydrophilic and therefore preferentially resides in water, and the other end is hydrophobic and preferentially resides in air.

Very weak (no film)	Weak (unstable)	Strong (stable w C16)	Very strong (C16 cpd dissolve)
Hydrocarbon	$-CH_2OCH_3$	$-CH_2OH$; $-C_6H_4OH$	$-SO_3^-$
$-CH_2I$	$-C_6H_4OCH_3$	$-CN$; $-CH_2COCH_3$	$-SO_4^-$
$-CH_2Br$	$-COOCH_3$	$-COOH$; $-NHCONH_2$	$-C_6H_4SO^{4-}$
$-CH_2Cl$		$-CONH_2$	$-NR_4^+$
$-NO_2$		$-CH=NOH$	

Table 1

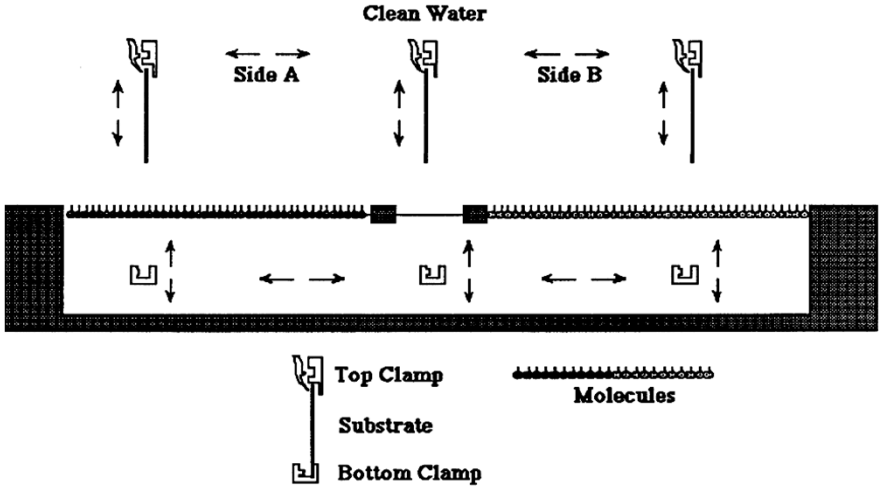

Figure 4. A cross-section view of LB film deposition in the KSV 5000 trough.

The deposition cycle in the KSV 5000 trough.

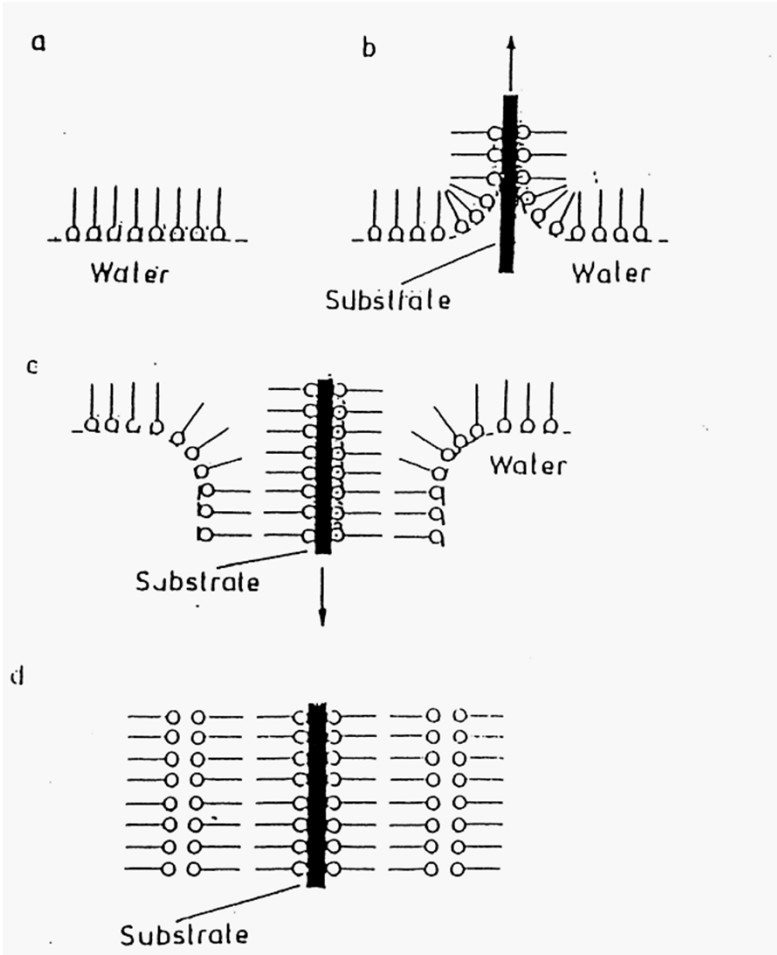

Figure 5. Y-type Langmuir-Blodgett film deposition.

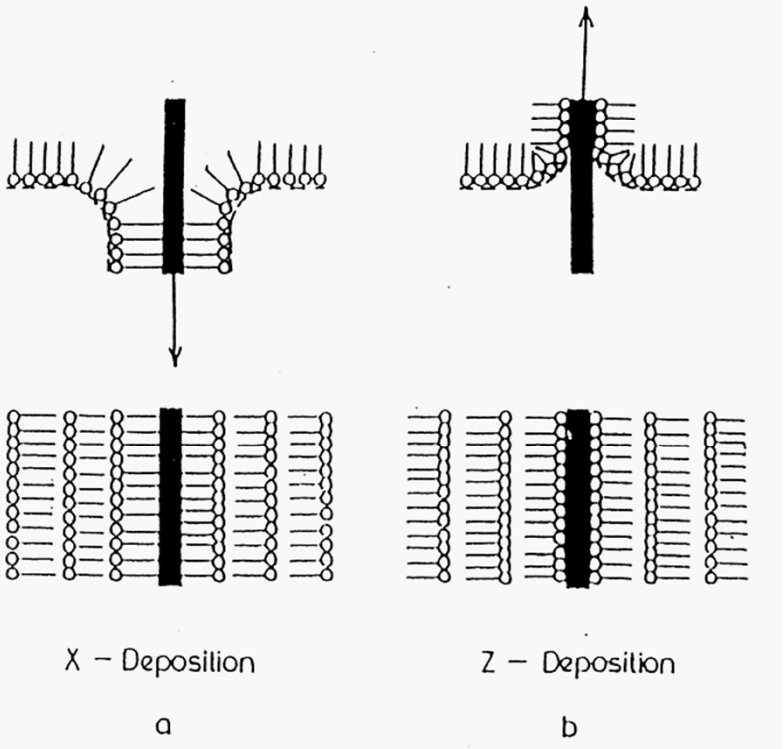

Figure 5-1. (a) X-type deposition. (b) Z-type deposition.

L-B films provide a way to control the packing density, molecular separation and position in a monolayer.

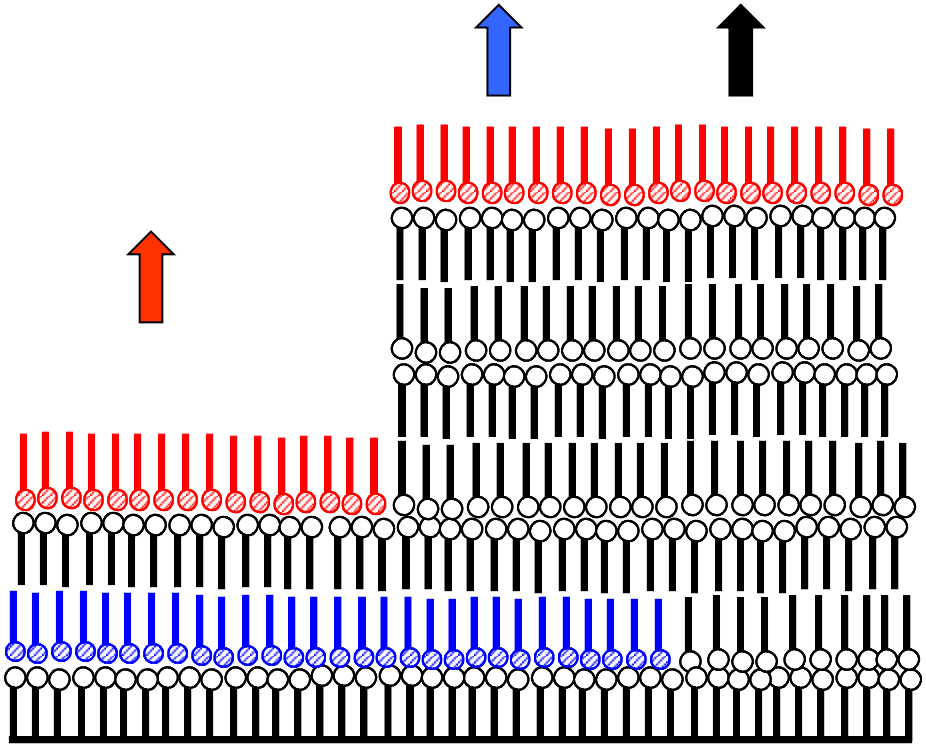

UV light

S

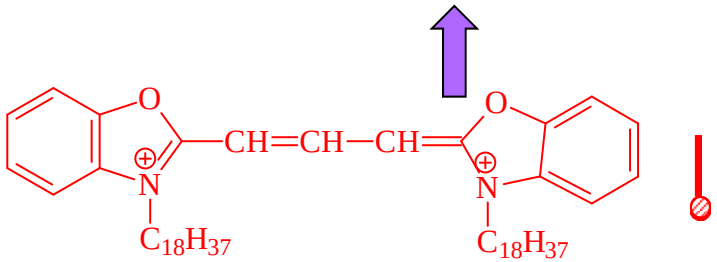

A

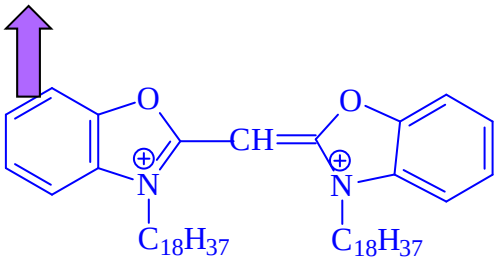

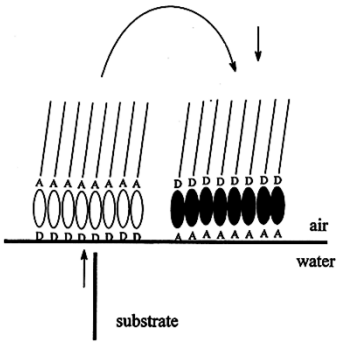

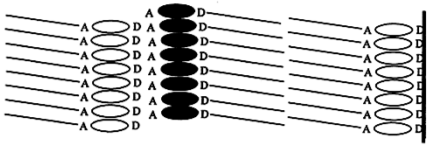

Figure 6.

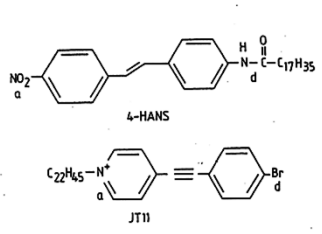

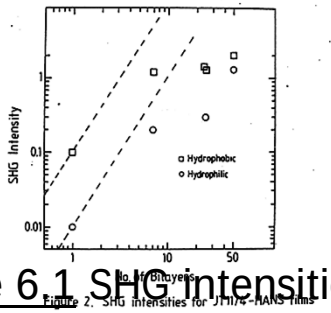

Figure 6.1 SHG intensities for JT11/4-HANS films.

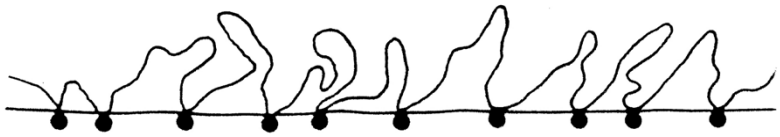

Figure 7. A polymer with widely spaced hydrophilic groups will form irregular loops on water surface

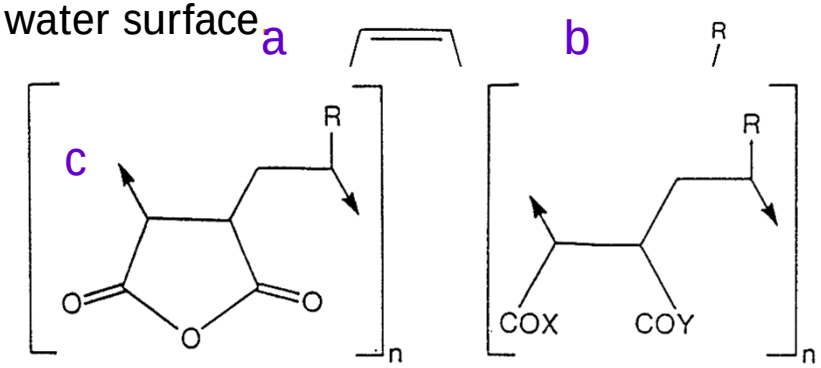

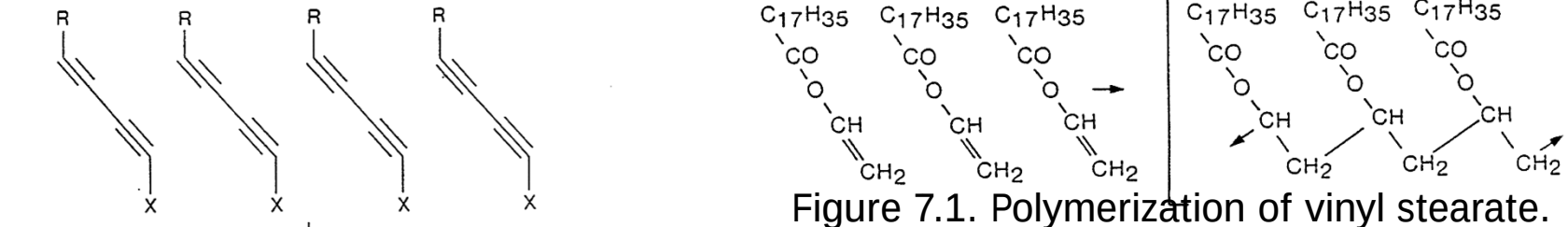

Figure 7.1. Polymerization of vinyl stearate.

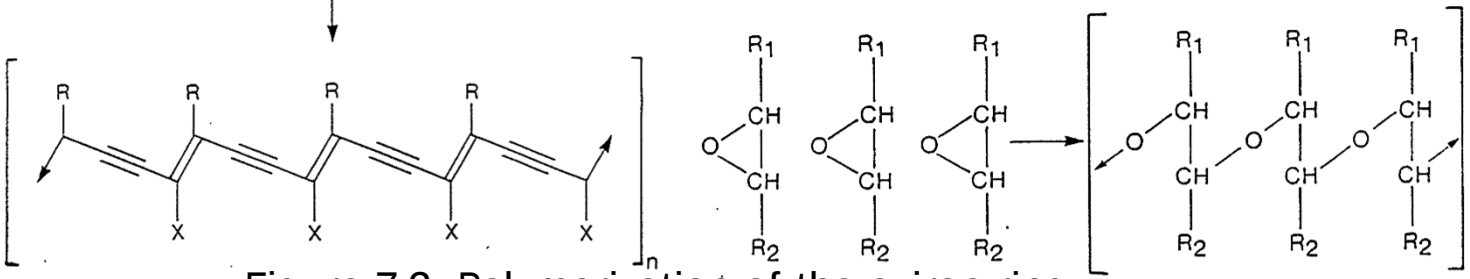

Figure 7.2. Polymerization of the oxiran ring.

- Self-assembly is the spontaneous organization of molecules or objects into stable, well-defined structures by non-covalent forces.

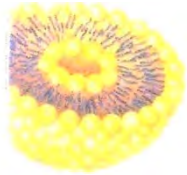

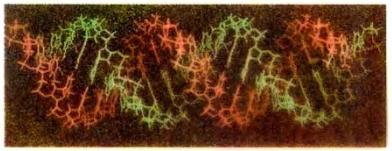

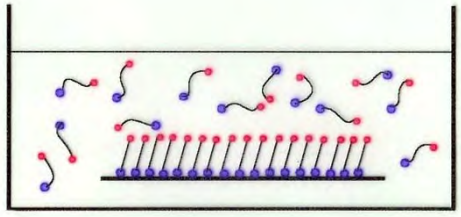

- Self-assembled monolayer (SAM) is the special case in which long-chain, functionalized molecules self-organize at a solid surface after chemisorption.

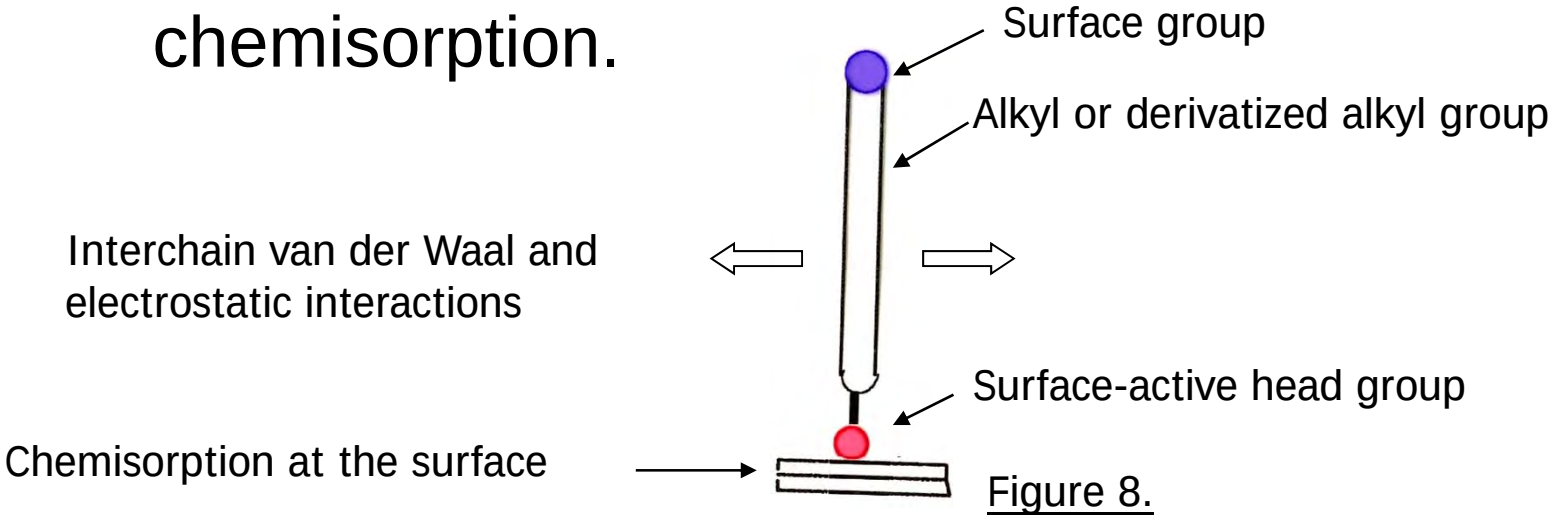

Figure 8.

Substrates and Ligands that form SAMS.

Substrate	Ligand or Precursor	Binding
Au	RSH, ArSH (thiols)	RS-Au
Au	RSSR' (disulfide)	RS-Au
Au	RSR' (sulfides)	RS-Au
Au	RSO_2H	RSO_2-Au
Au	R_3P	R_3P-Au
Ag	RSH, ArSH	RS-Ag
Cu	RSH, ArSH	RS-Cu
Pd	RSH, ArSH	RS-Pd
Pt	RNC	RNC-Pt
GaAs	RSH	RS-GaAs
InP	$RSiCl_3$,$RSi(OR')_3$	RS-InP

Substrate	Ligand or Precursor	Binding
SiO_2,glass	$RSiCl_3$, $RSi(OR')_3$	Siloxane
Si/Si-H	$(RCOO)_2$ (neat)	R-Si
Si/Si-H	$RCH=CH_2$	RCH_2CH_2Si
Si/Si-Cl	RLi,RMgX	R-Si
Metal oxides	RCOOH	$RCOO^-$ …MO_n
Metal oxides	RCONHOH	RCONHOH …Mo_n
ZrO_2	RPO_3H_2	RPO_3^{2-}…Zr^{IV}
In_2O_3/SnO_2 (ITO)	RPO_3H_2	RPO_3^{2-}…M^{n+}

Table 2.

- Advancing contact angles θ_a of water and hexadecane on mono-layers or representative thiols on gold.

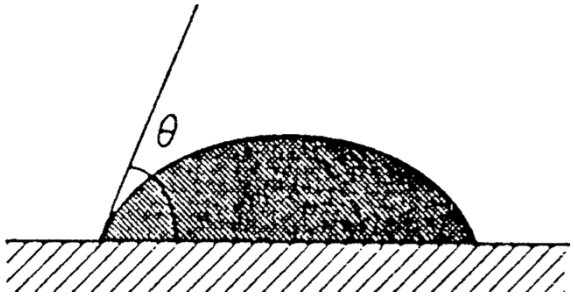

Thiol	Θ_a (H2O) (o)	Θ_a ($C_{16}H_{34}$) (o)	Thiol	Θ_a (H2O) (o)	Θ_a ($C_{16}H_{34}$) (o)
$HS(CH_2)_2(CF_2)_5CF_3$	118	71	$HS(CH_2)_{16}OCH_3$	75	41
$HS(CH_2)_{17}CH_3$	112	47	$HS(CH_2)_{10}CO_2CH_3$	67	28
$HS(CH_2)_{17}CH=CH_2$	107	39	$HS(CH_2)_{11}CN$[b]	63	<5
$HS(CH_2)_{19}Br$[a]	97	<5	$HS(CH_2)_{10}CONH_2$[c]	13	<5
$HS(CH_2)_{14}OCOCF_3$[d]	96	62	$HS(CH_2)_{15}CO_2H$	<10	<5
$HS(CH_2)_{19}F$[a]	95	<5	$HS(CH_2)_{11}OH$	<10	<5
$HS(CH_2)OCH_3$	83	<5			

Table 3.

Infrared Reflection Absorption Spectroscopy (IRRAS)

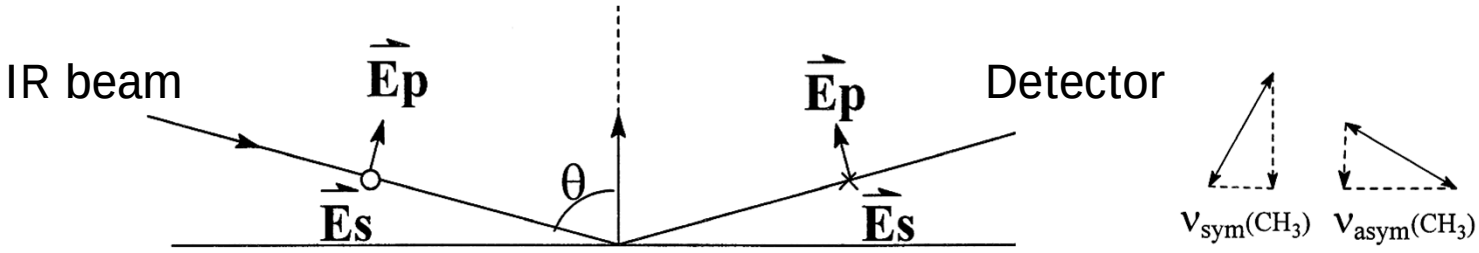

- For Reflective surfaces such as metal:

The vector sum of $\vec{E}s$ at surface approaches 0,

The vector sum of $\vec{E}p$ varies with incidence angle θ

$$I \propto \left| \frac{\partial \vec{\mu}}{\partial q} \cdot \vec{E} \right|^2 \propto \cos^2\alpha = \frac{I_{obs}}{3I_{calc}}$$

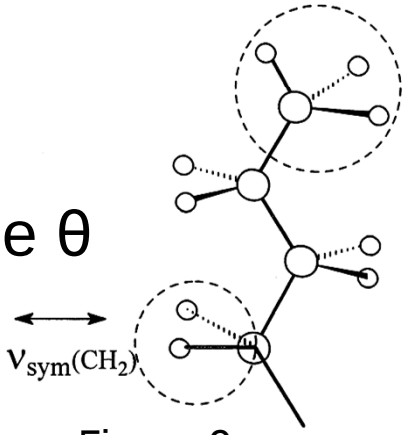

Figure 9.

α: angle between $\vec{E}p$ and the direction of transition dipole

Figure 10. Proposed structure for n-Alkanoic acid on Silver

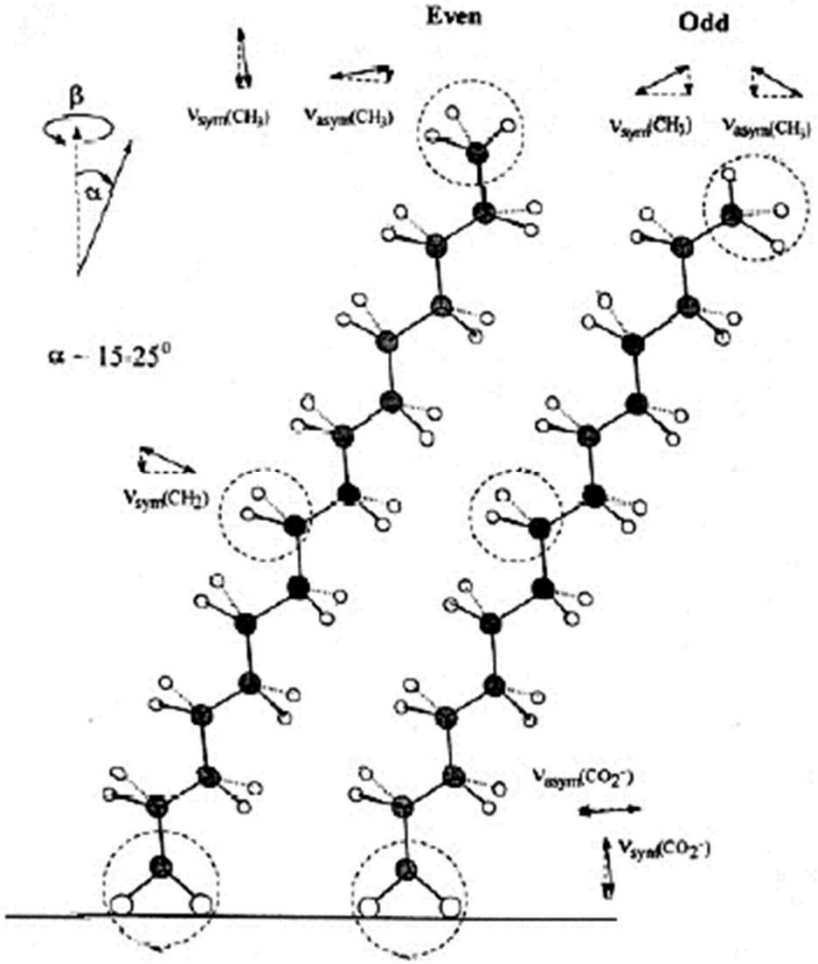

Figure 10.1. Proposed structure for n-Alkanoic acid on Aluminum and Copper

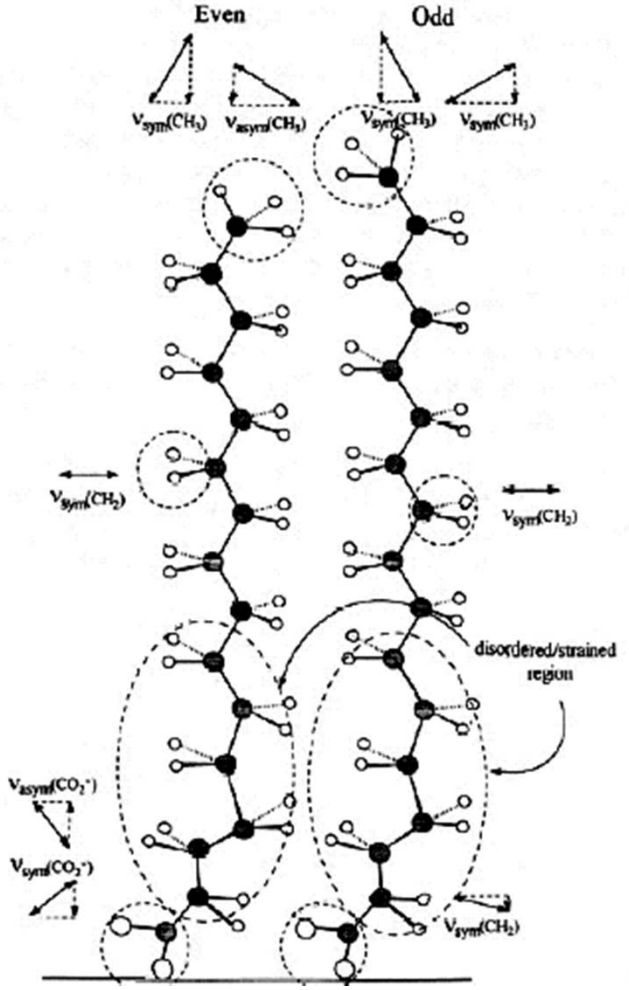

Tao, Y.T. *J. Am. Chem. Soc.* 1993, V. 115 (10) P. 4356

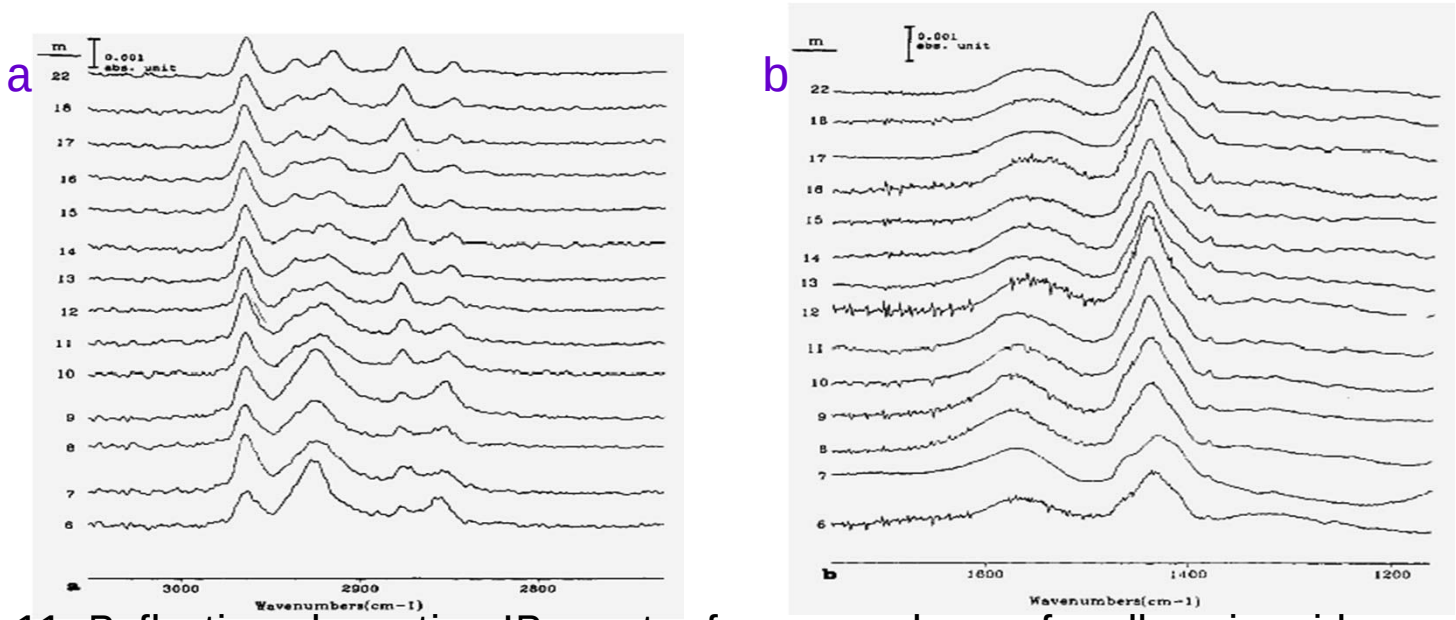

Figure 11. Reflection-absorption IR spectra for a monolayer of n-alkanoic acid, $CH_3(CH_2)_mCOOOH$ on Cu. (a) High-frequency region. (b) Low-frequency region.

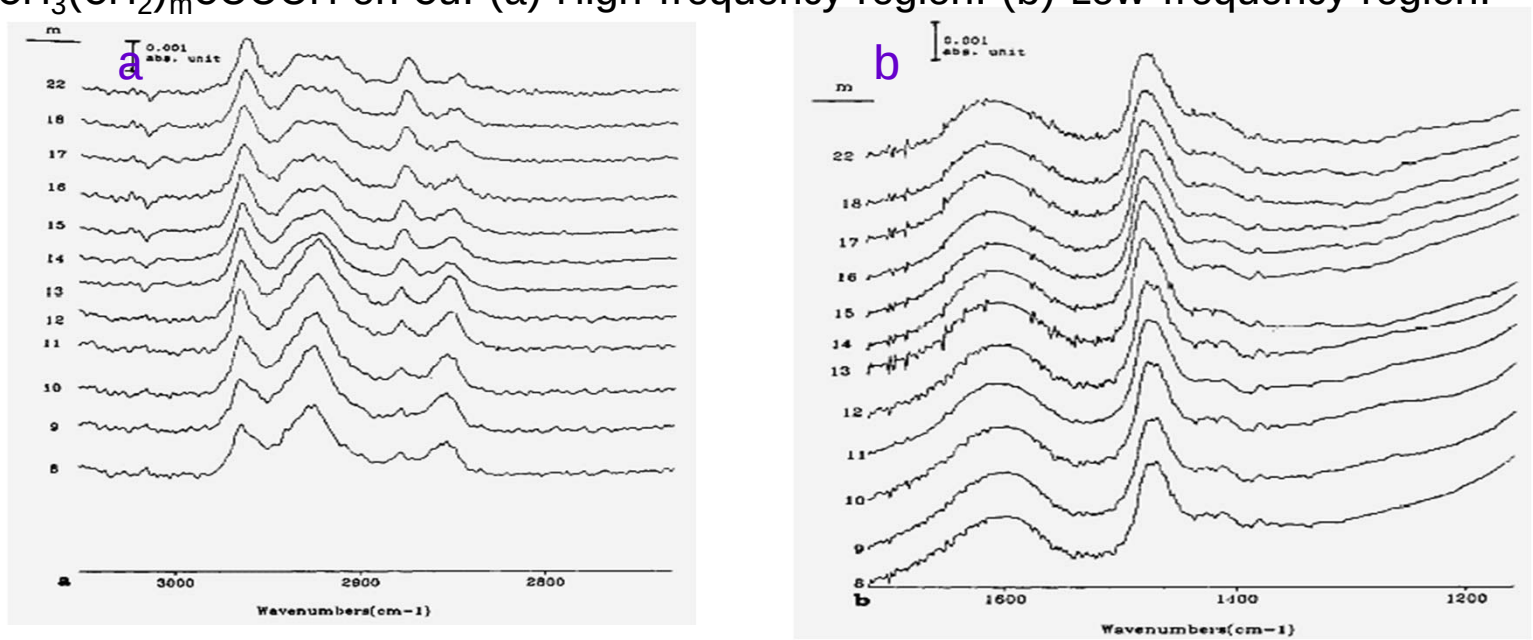

Figure 11.1. Reflection-absorption IR spectra for a monolayer of n-alkanoic acid, $CH_3(CH_2)_mCOOOH$ on Al. (a) High-frequency region. (b) Low-frequency region.

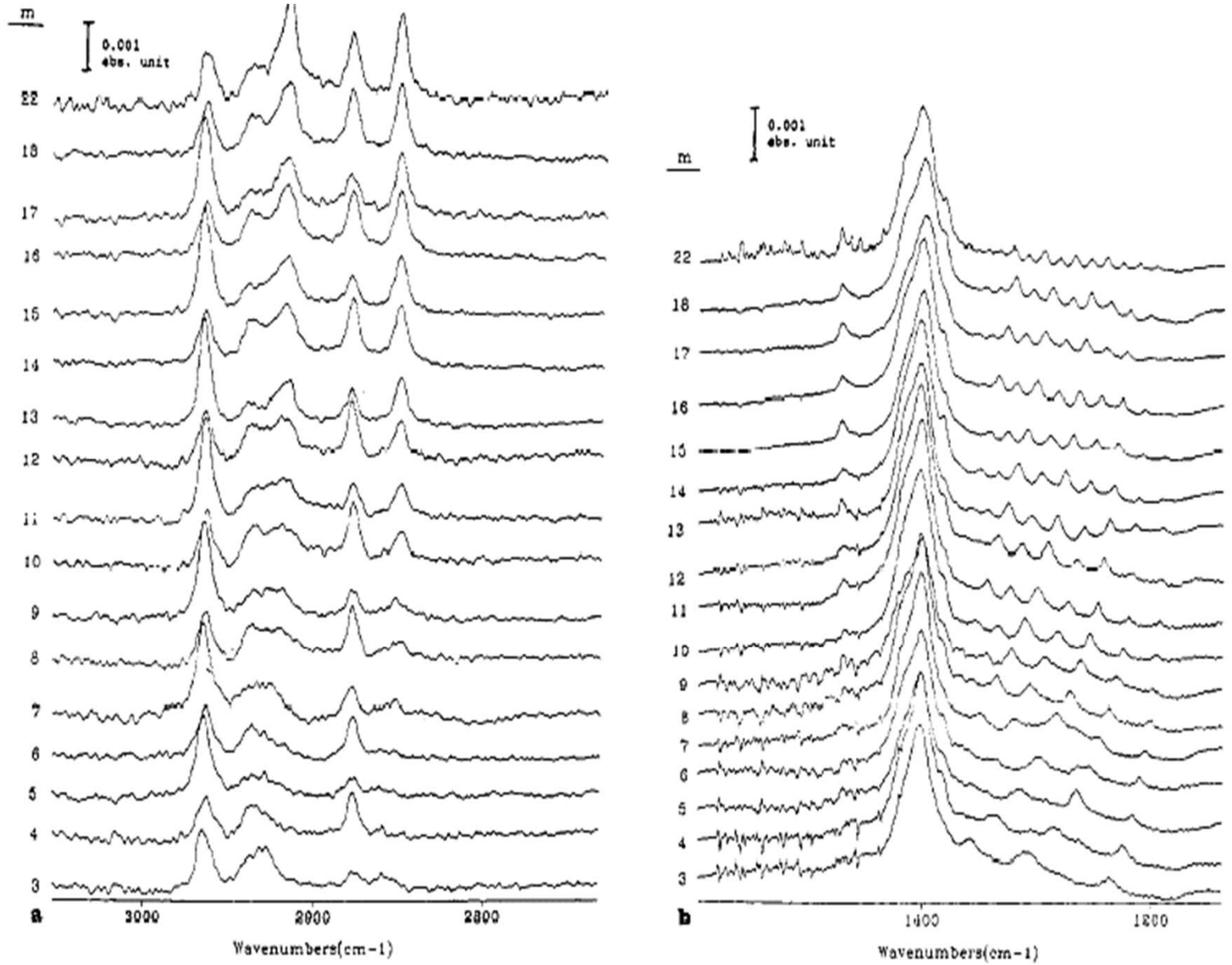

Figure 12. Reflection-absorption IR spectra for a monolayer of n-alkanoic acid, $CH_3(CH_2)_mCOOOH$ on Ag. (a) High-frequency region. (b) Low-frequency region.

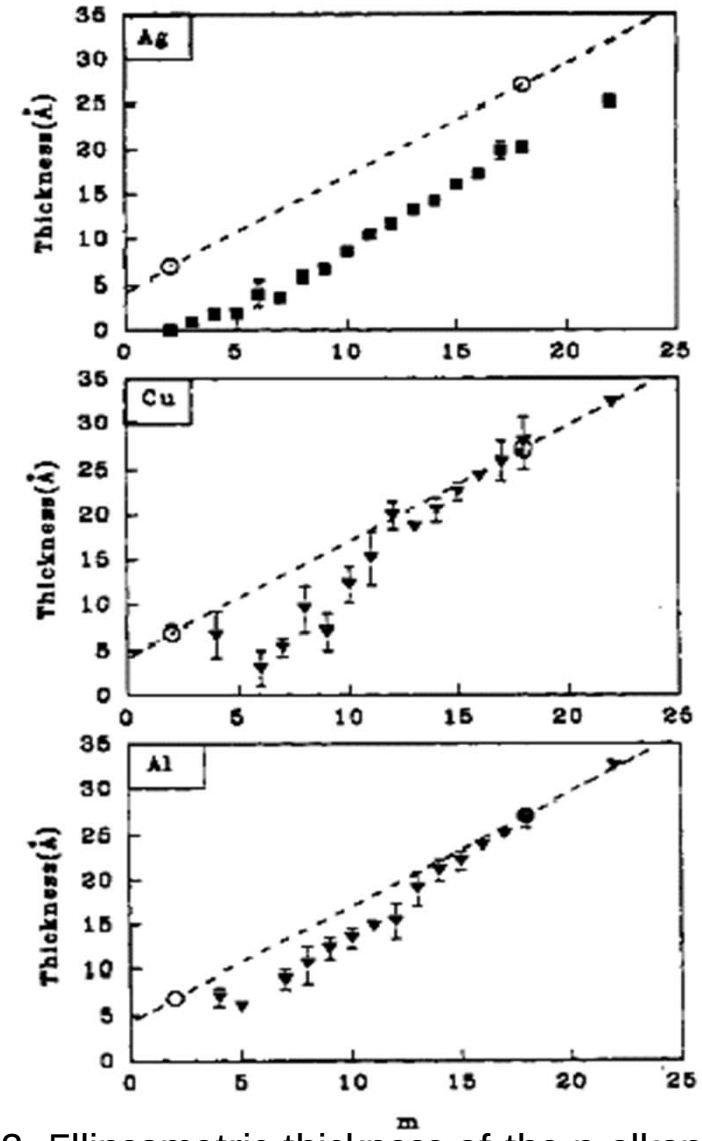

Figure 13. Ellipsometric thickness of the n-alkanoic acid monolayer as a function of chain length. Dashed line represents the calculated thickness for normal orientation.

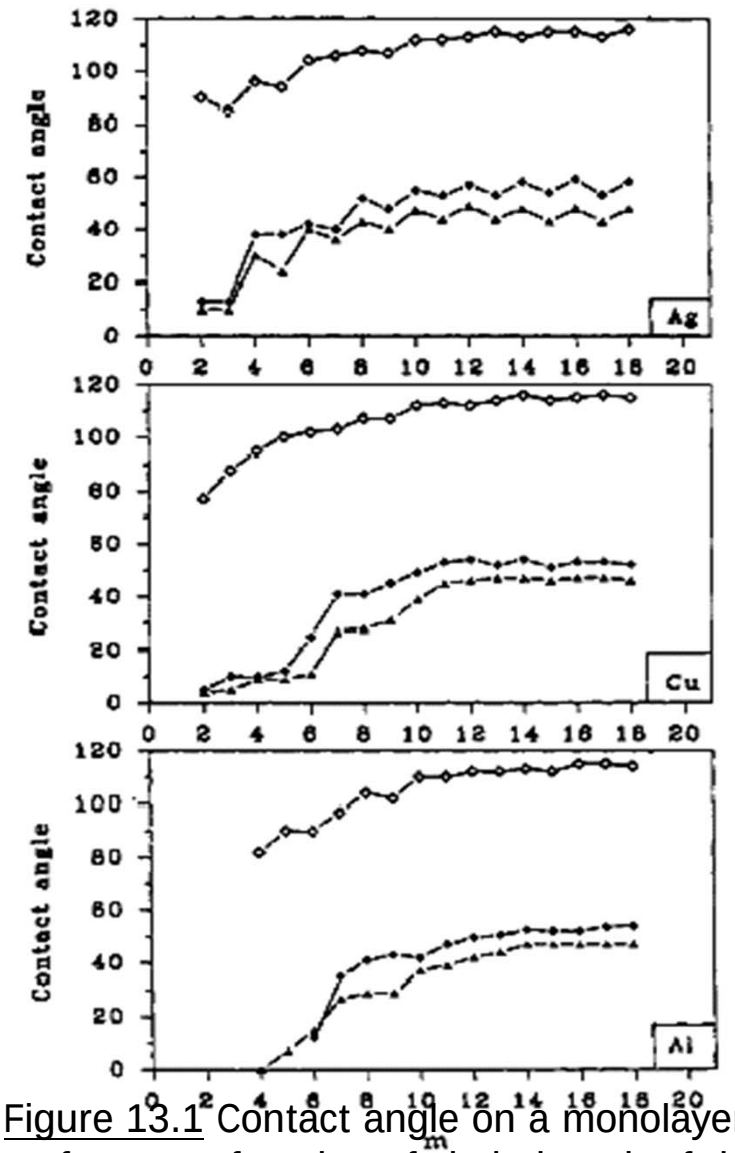

Figure 13.1 Contact angle on a monolayer surface as a function of chain length of the acid: (Δ)hexadecane, (⧫)bicyclohexyl, (◊)water.

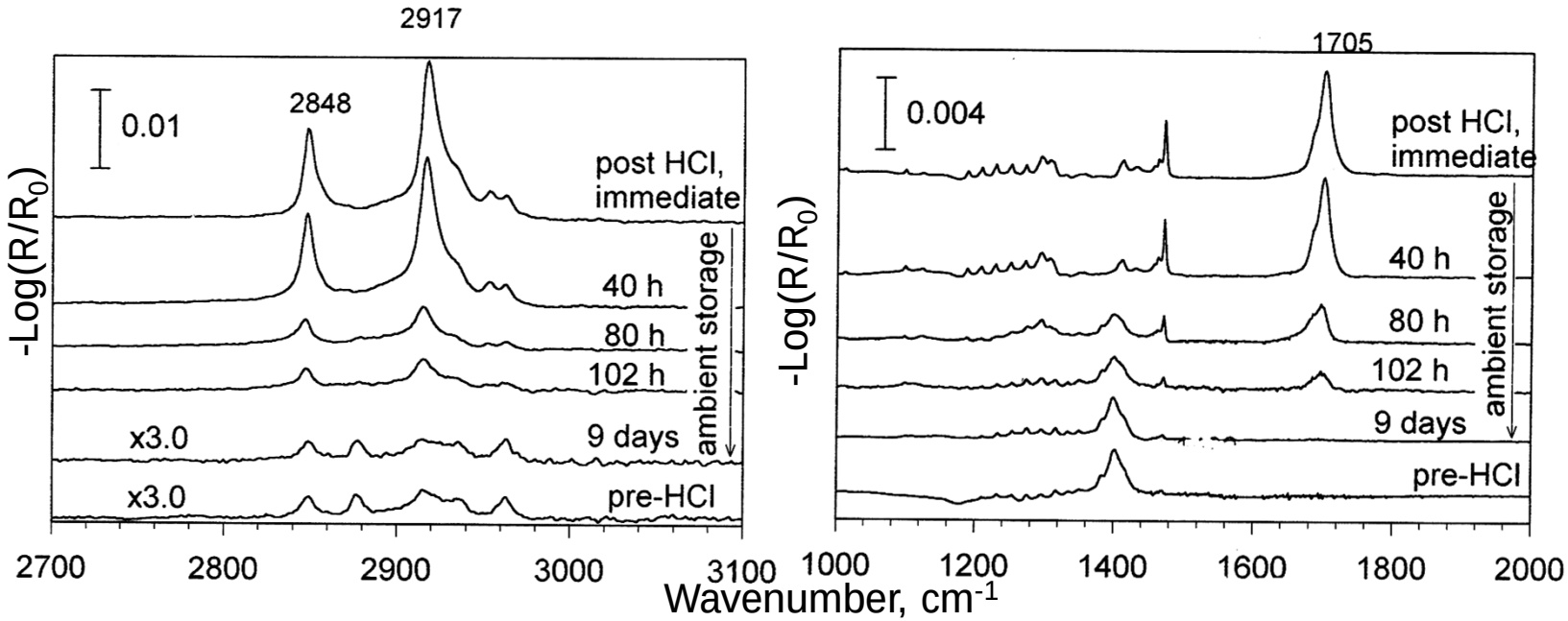

Figure 14. SAM of n-hexadecanoic acid on Ag before and after exposure to HCl vapor for 10 sec.

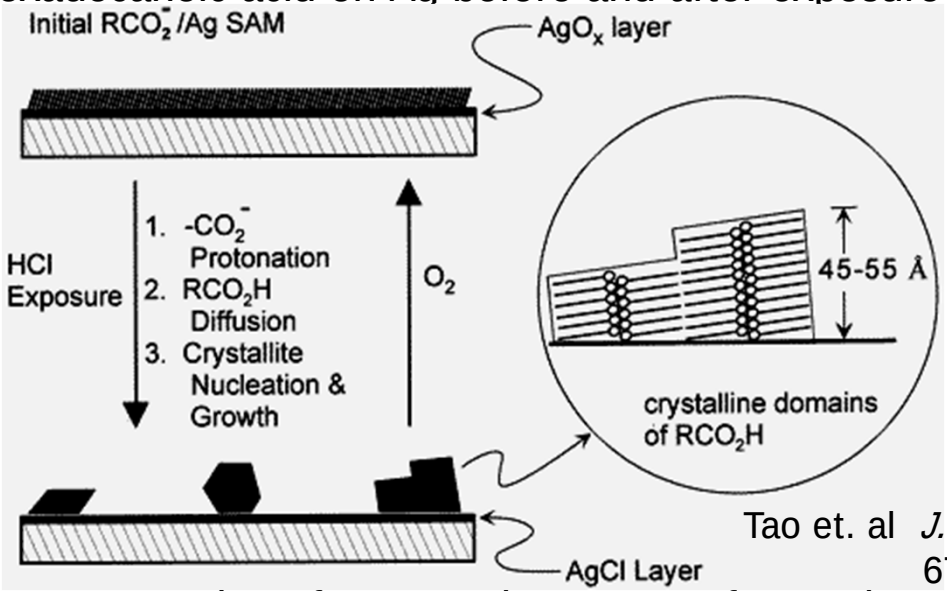

Tao et. al *J. Am. Chem. Soc*. 118 , 6724 (1996).

Figure 14.1 Schematic representation of proposed structures for a *n*-hexadecanoic acid monolayer on Ag before and immediately after a 10-s HCl exposure.

General Reaction Mechanism

- RCO_2^-(2-D,c)/M[oxide]/M + HCl(g) ---> RCO_2H*(2-D,c)/M[Cl^-]/M
- RCO_2H*(2-D,c)/M[Cl^-]/M---------- > RCO_2H*(3-D,c)/M[Cl^-]/M
- RCO_2H*(3-D,c)/M[Cl^-]/M + O_2(g) ---- > RCO_2H*(3-D,c) / [oxide] /M
- RCO_2H*(3-D,c)/M[oxide]/M ----------> RCO_2^-(2-D,c)/M[oxide]/M

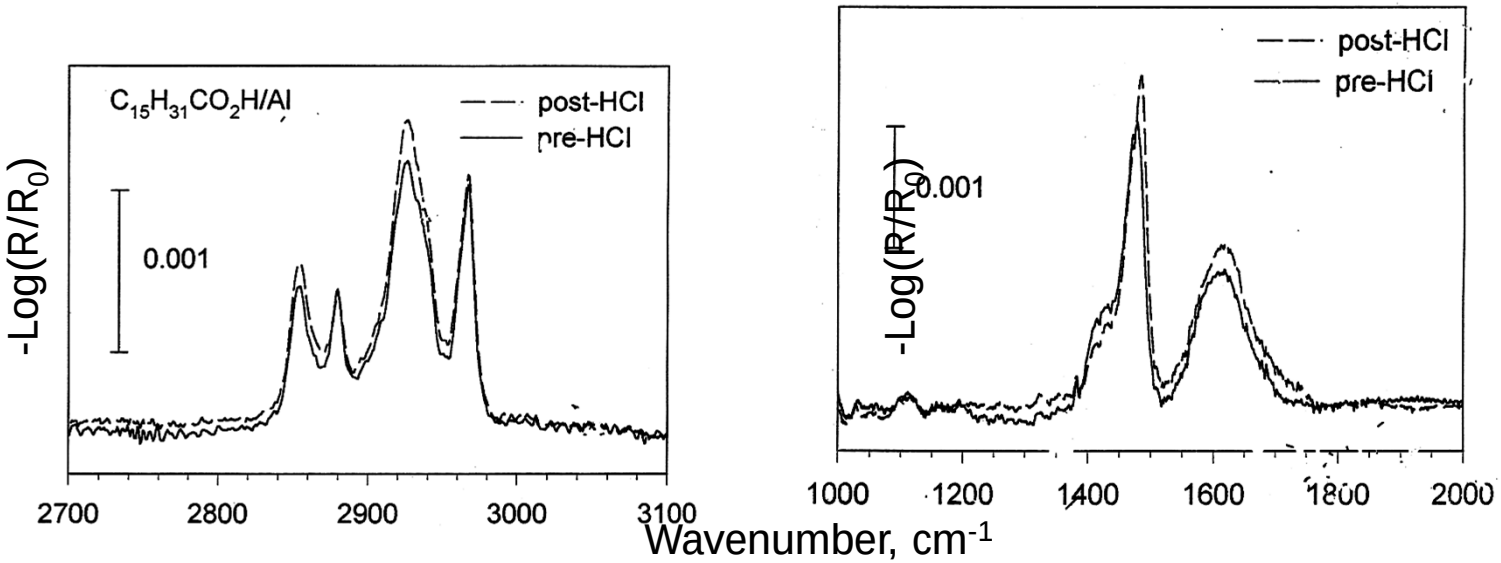

Figure 15. n-hexadecanoic acid monolayer on Al before and after HCl exposure

Figure 16. H_2S Induced Reorganization of Self-Assembled Monolayer of n-Alkanoic Acid

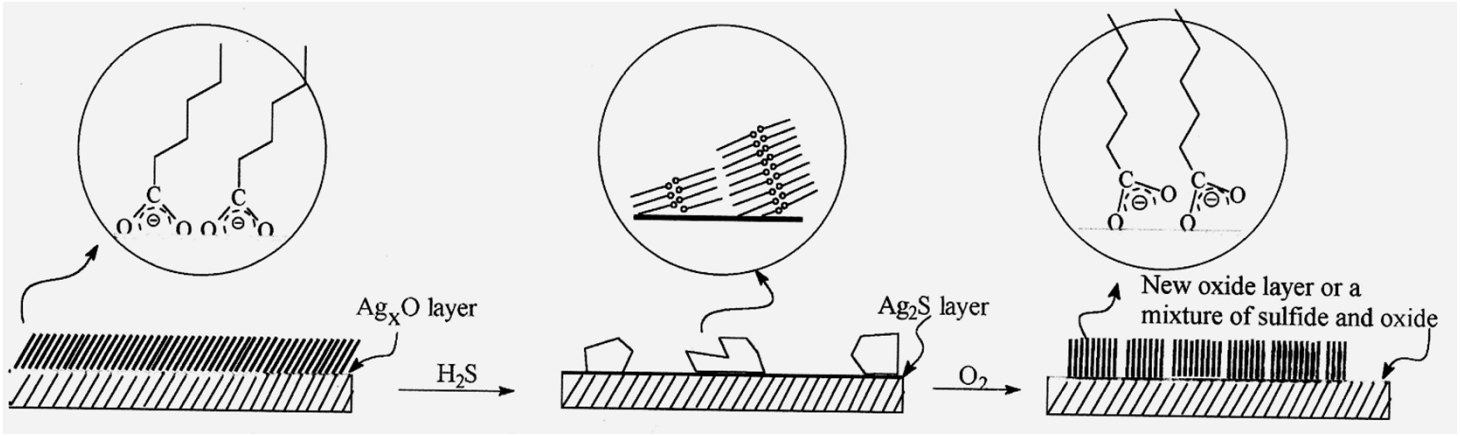

Tao, Y.T. *J. Phys. Chem. B*, 101, 9732(1997).

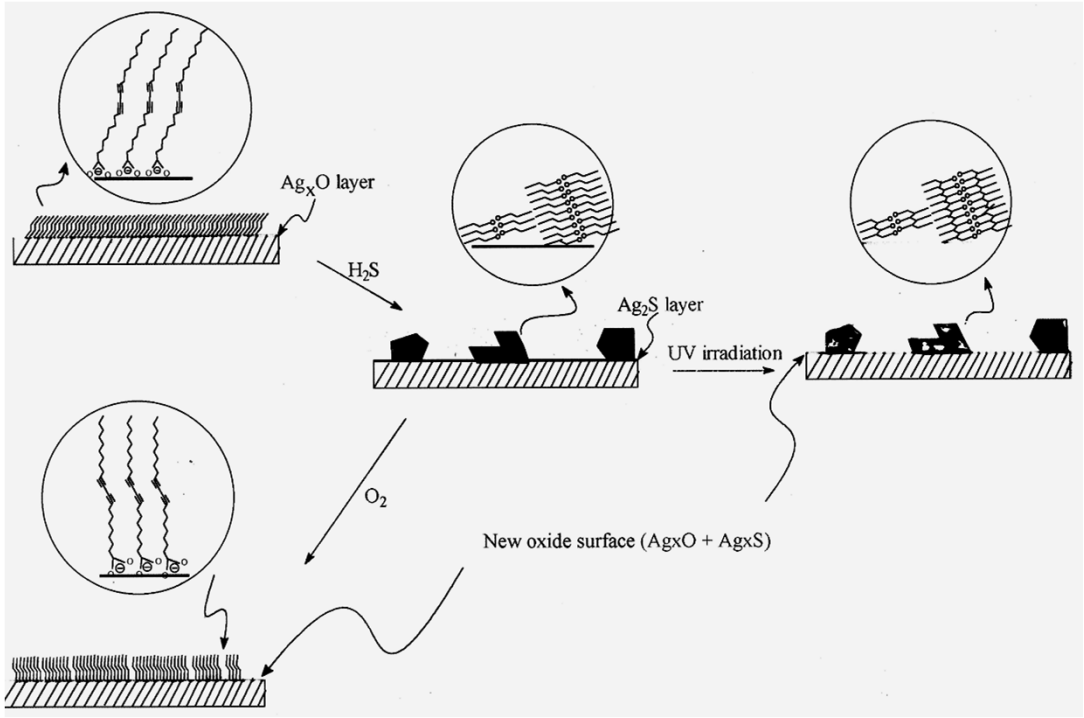

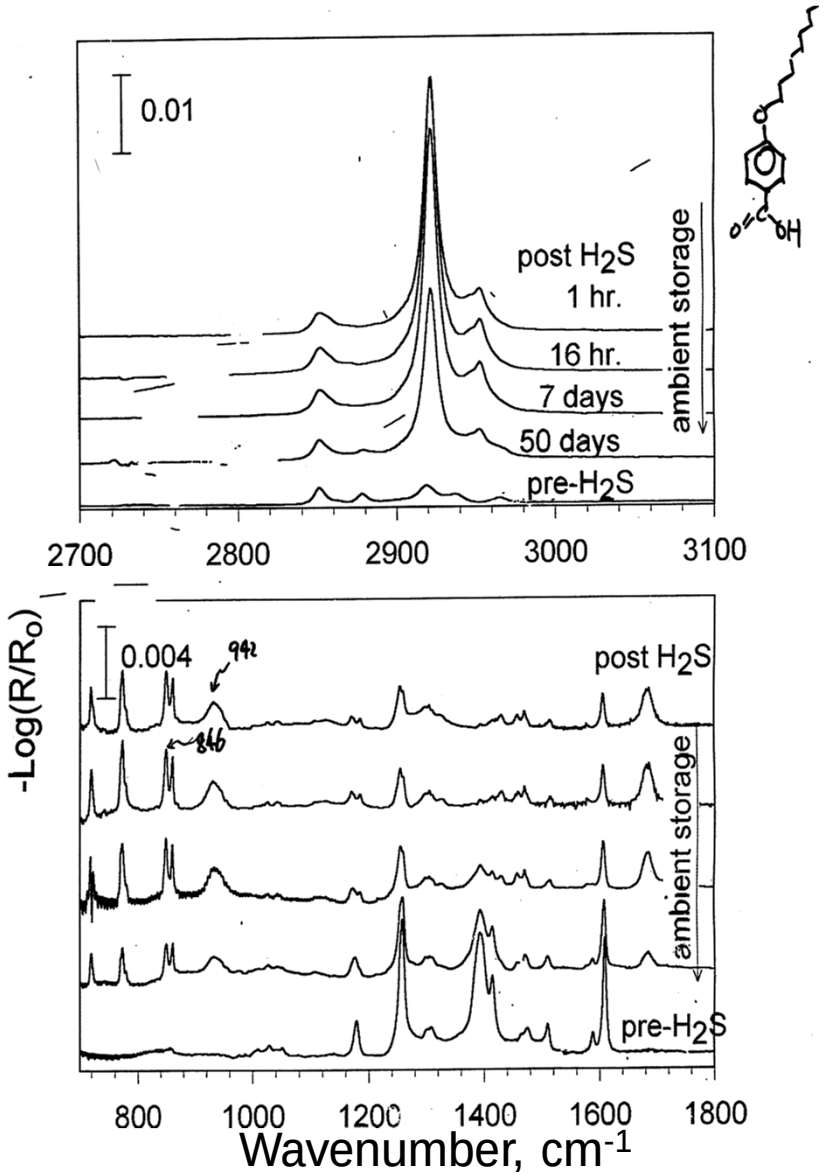

Figure 17. External reflection IR for C16-derivatized benzoic acid monolayer on Ag, before and after H2S exposure.

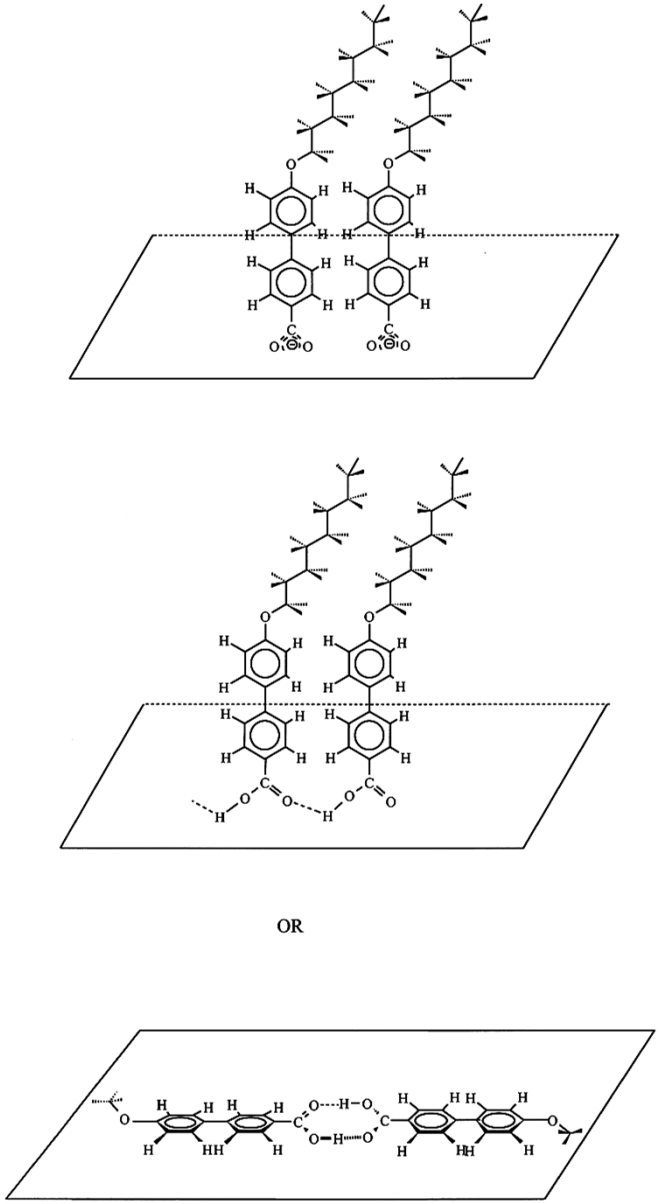

Figure 17.1

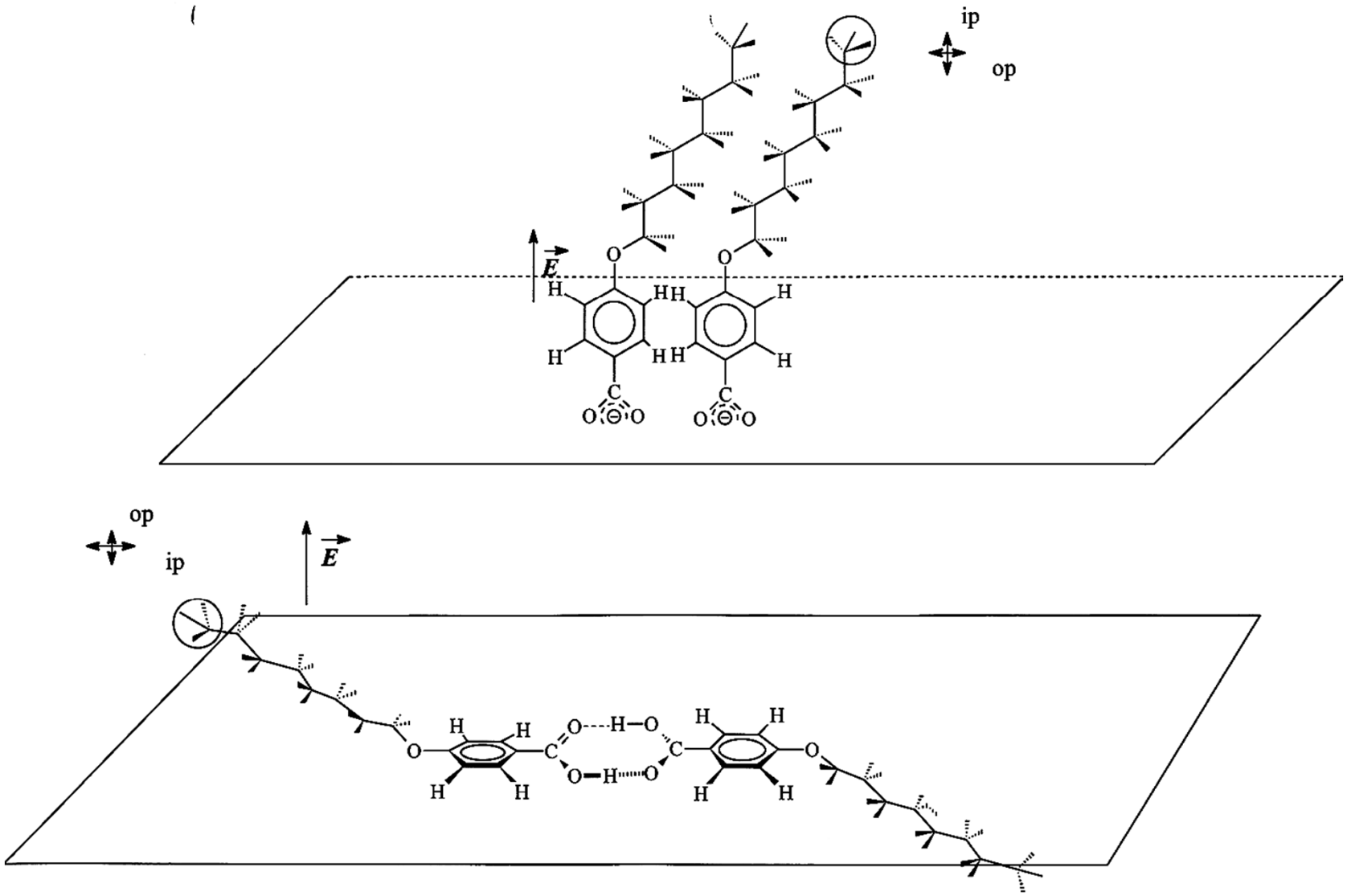

Figure 17.2

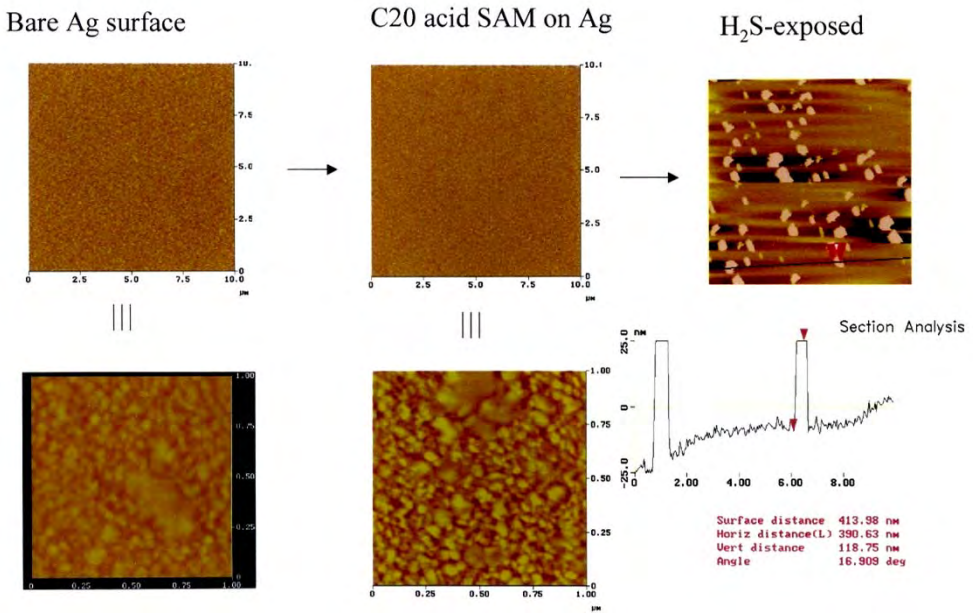

Figure 18.

Figure 18.1 Restoration of monolayer of eicosanoic acid on Ag surface at 38°C, completed in 90 min.

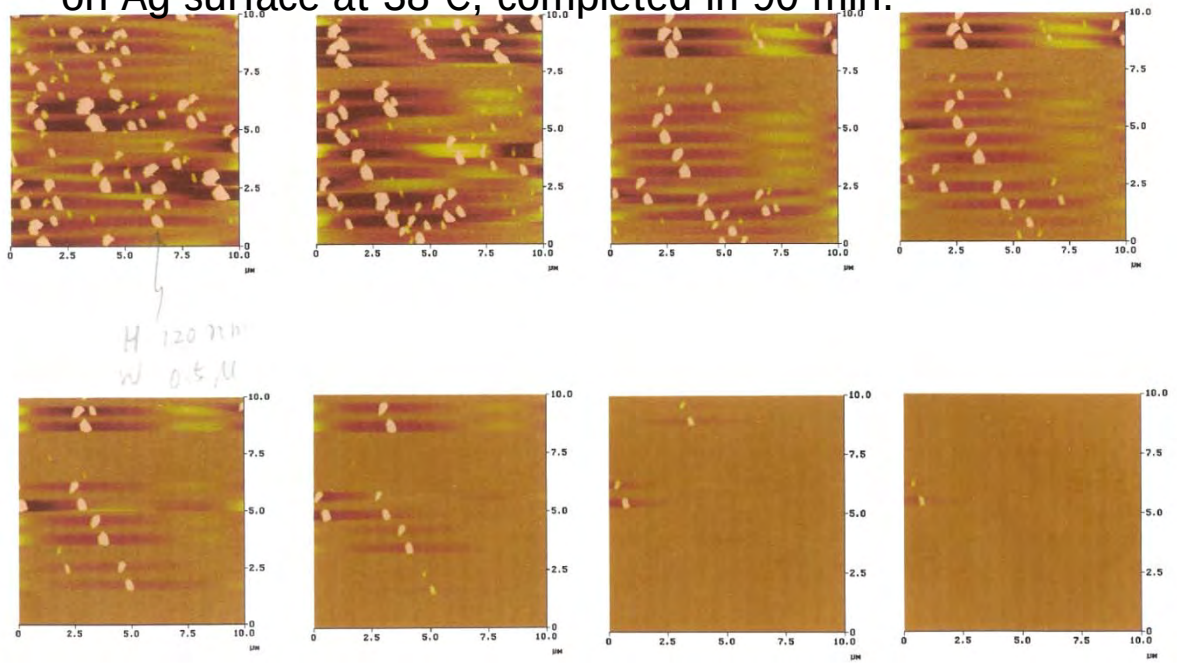

Figure 18.2 Restoration of monolayer of 4-hexadecyloxybenzoic acid on Ag surface

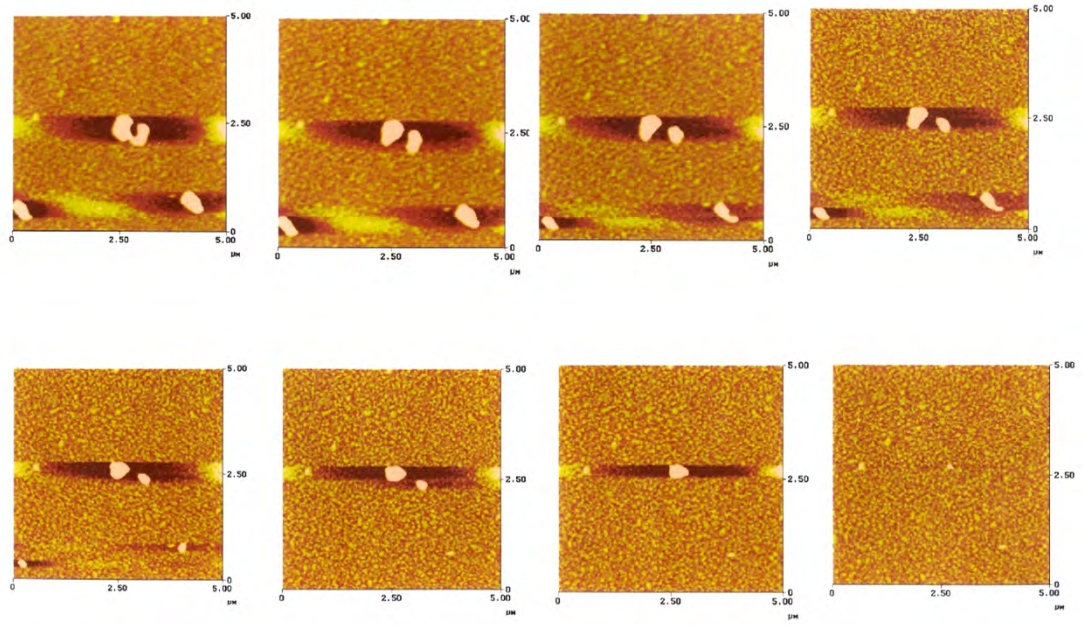

Figure 19. Schematic representation of the structure of a thioacid monolayer on Ag and Au before and after hydrolysis

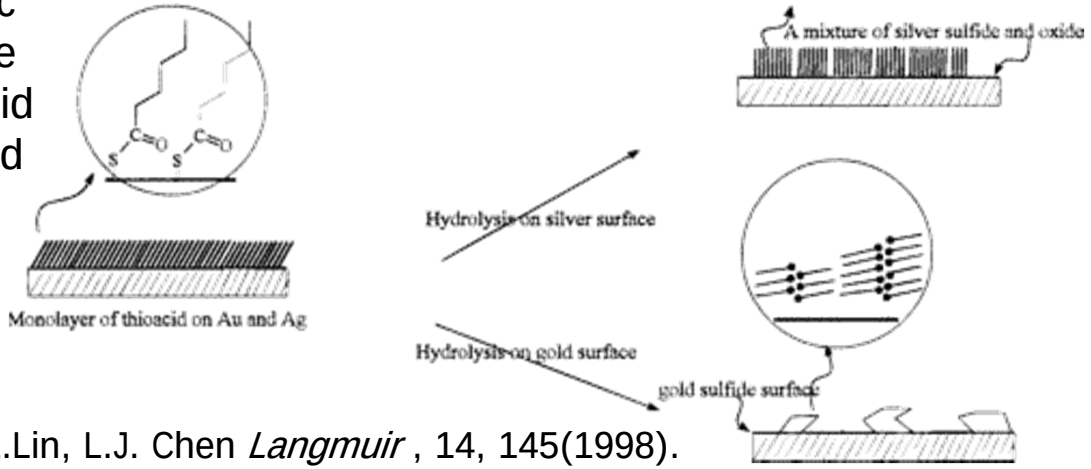

Y.T.Tao, S. Pandiaraju, W.L.Lin, L.J. Chen *Langmuir* , 14, 145(1998).

Adsorption of Alkyltrichlorosilane on Hydroxylated Surface

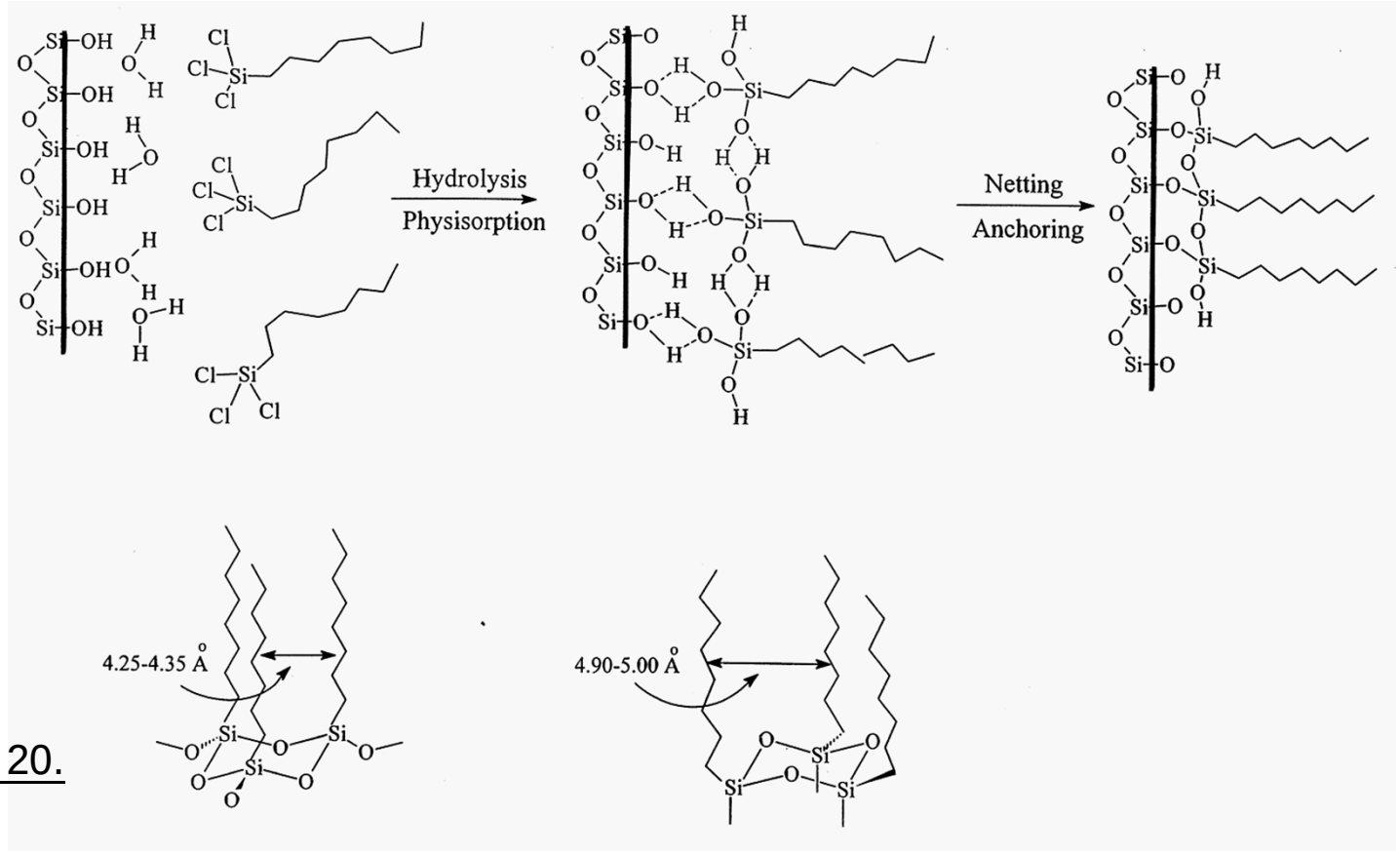

Figure 20.

Alkanethiol on gold and silver surfaces

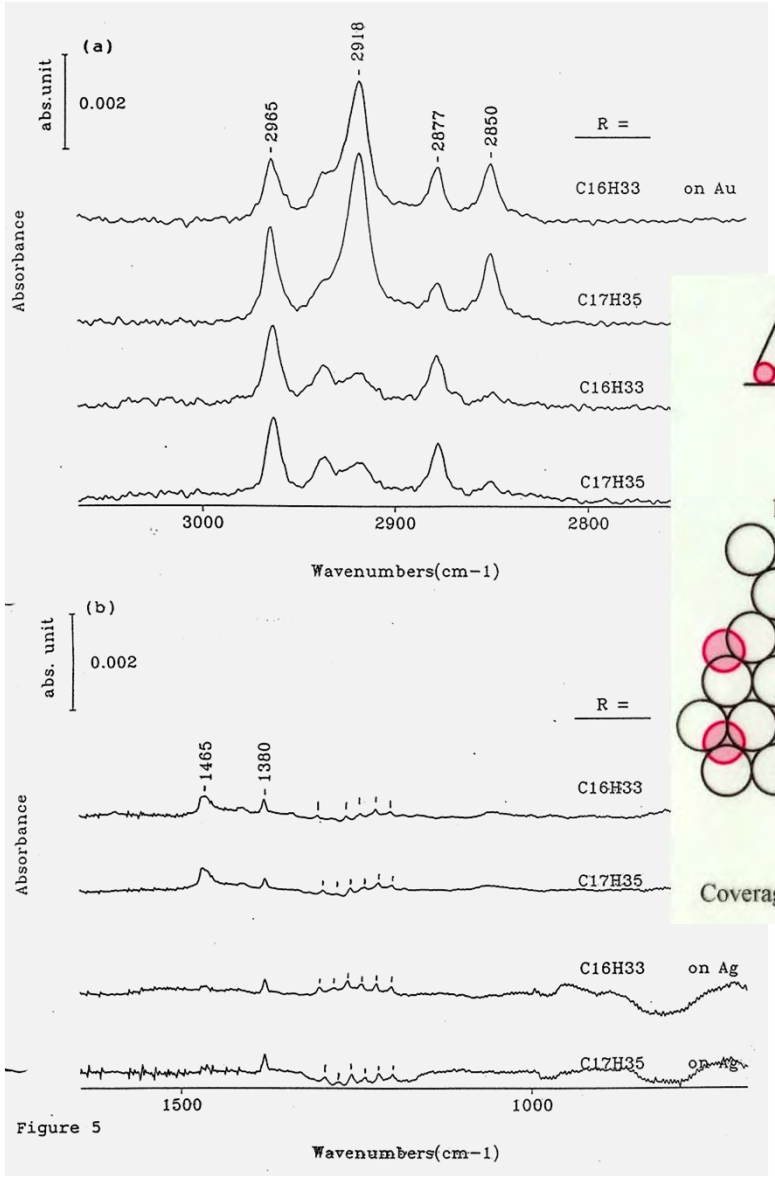

Figure 5

Figure 21.

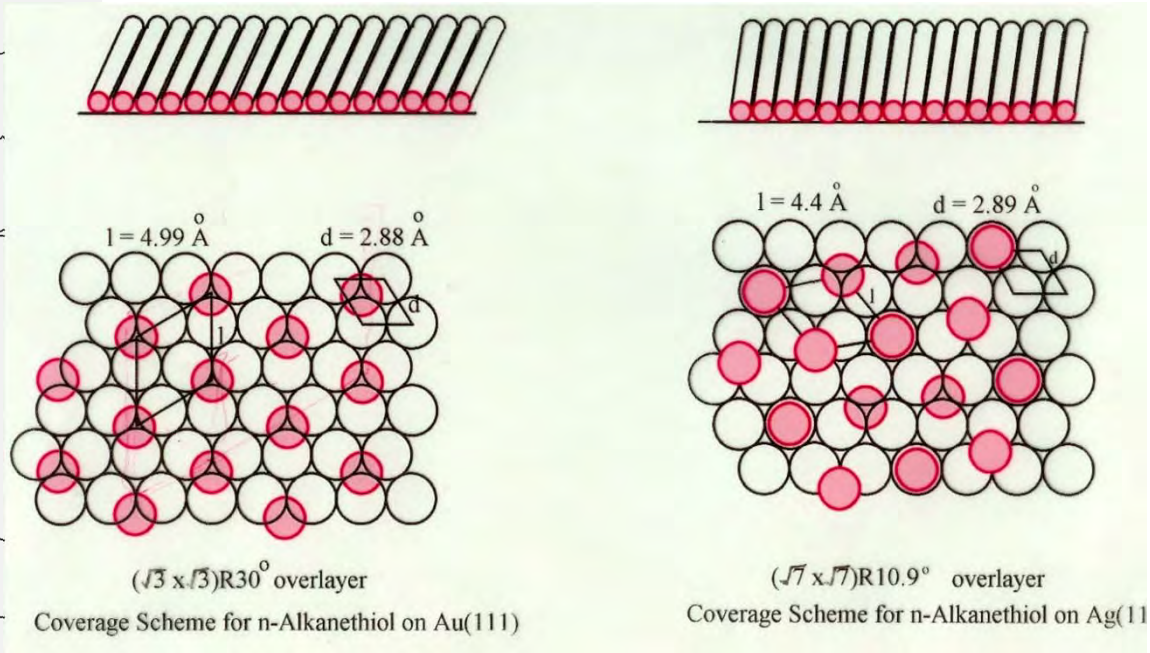

Why Alkanethiolate SAMs on Au(111) and Ag(111) are Different?

1 X 3 assembly at 4.2-Å spacing (left), representing alkanethiolate on Ag(111), and at 4.97 Å-spacing (right), representing alkanethiolate on Au(111).

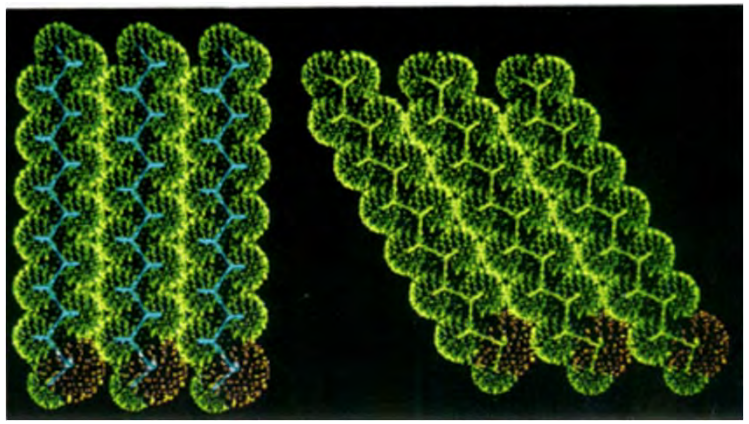

Best interaction energy (for optimal in-plane tilt) *as* a function of the spacing (d).

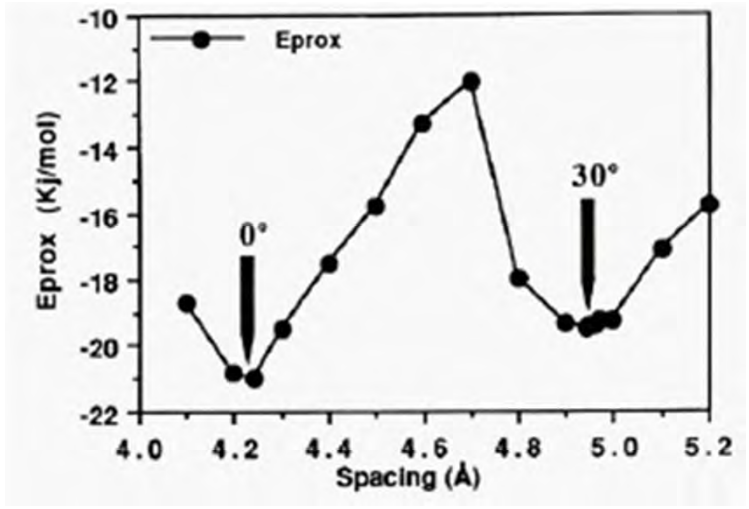

Ulman, A.; Eilers, J. E.; Tillman, N. *Langmuir*, *5,* 1147(1989).

Why are Alkanethiolates on Au(111) and Ag(111) Different?

Facts:

1. **The nearest-neighbor distance for Au(111) and Ag(111) lattices are similar (2.88 and 2.89 Å, respectively.)**
2. **Iodine forms a ($\sqrt{3}\times\sqrt{3}$)R30° structure on Ag(111), with the iodine atoms occupying the hollow sites.**

Difference between of alkanethiolate SAMs on Au(111) and on Ag(111) must result from an interplay of chemisorption and chain-chain interactions:

1. **Silver is more reactive than gold, it forms an oxide spontaneously, its oxidation potential is 1.7 eV lower, and its work function 0.6 eV lower.**
2. **Gold and silver differs due to relativistic effects. The peak-to-valley roughness at their [111] lattices, 6.0 kcal mol^{-1} for Au(111) and only 3.3 kcal mol^{-1} for Ag(111). Site selection is more effective for Au(111).**

Why are Alkanethiolates on Au(111) and Ag(111) Different? - *Continued*

3. **Because in Ag(111) the energy difference is smaller than in Au(111), adsorption at an on-top site in the former may compete with that at the hollow site.**
4. **Only certain combinations of chain-chain separation and tilt angles permit truly effective packing of alkyl chains. The most effective packing is a trigonal lattice with spacing near 4.4 Å with a molecular axis normal to the surface. This distance (4.41 Å) was found for methanethiolate on Ag(111); however, for longer alkyl chains the distance of 4.6 Å has been reported. The second most effective has a spacing near 5.0 Å and the molecular axis tilted 30º, such that the distance between the chains is, again, 4.4 Å and the fit of bulges into depressions is again perfect.**
5. **Crowding more molecules per unit surface area will result in both more chemisorption energy and VDW attraction for the entire system simply because there are more chains involved. This is a lot of energy, since the possibility of adsorption at on-top sites means that in SAMs of thiolates on Ag(111) there are 26% more chains per unit area than on Au(111) on-top sites.**

Figure 22. AFM image of uncoated, epitaxially grown Au(111) on mica covering 3.02 nm*3.02 nm. The image was collected in a constant- force mode and was lightly filtered using an XY spectrum filter. The average nearest-neighbor spacing represented by line a equals 0.29±0.03nm, and the next-nearest-neighbor spacing represented by line b is 0.05±0.04 nm.

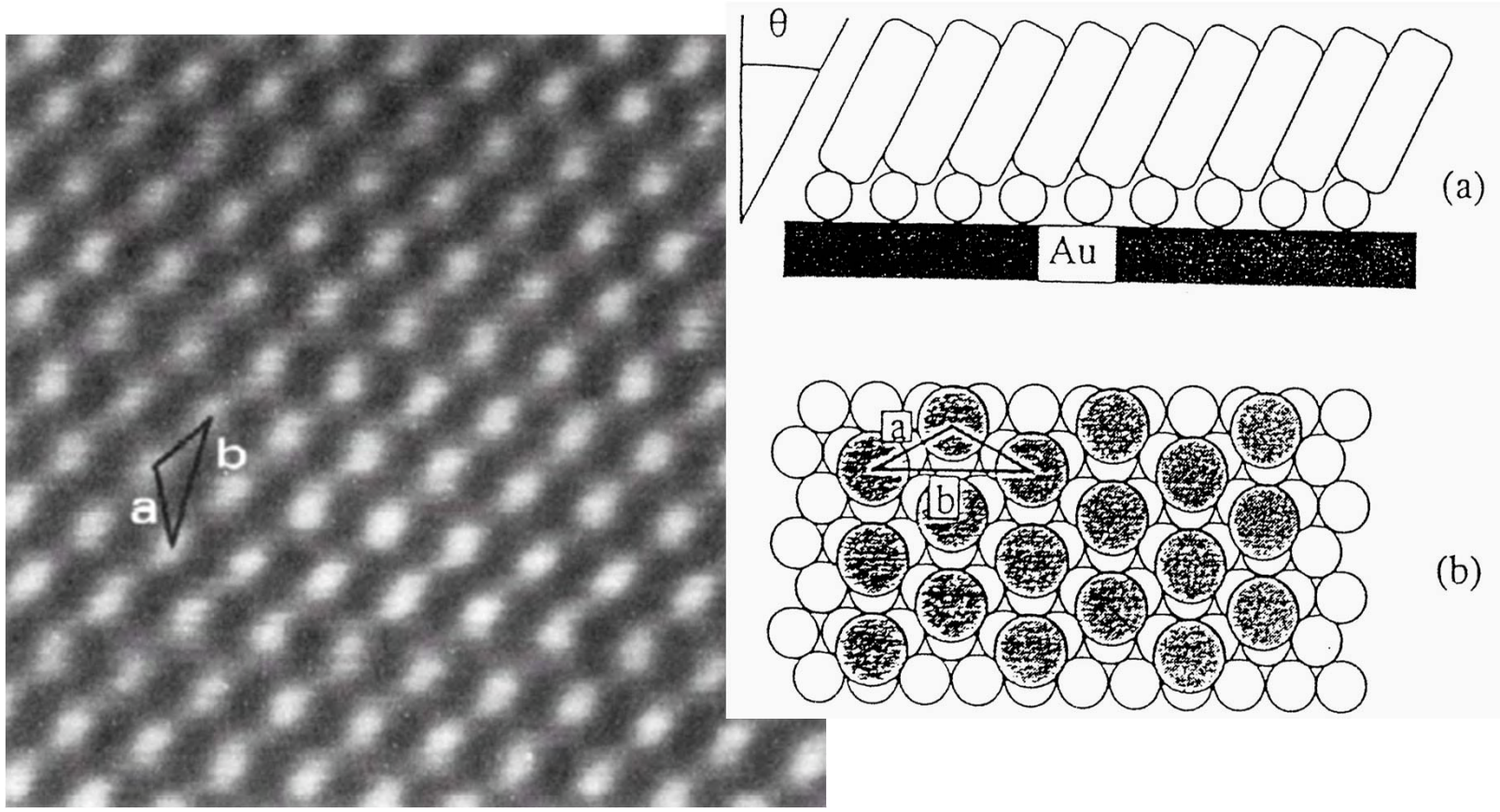

C.A. Alves, E.L Smith, M. D. Porter, *J. Am. Chem. Soc*. 114, 1223(1992).

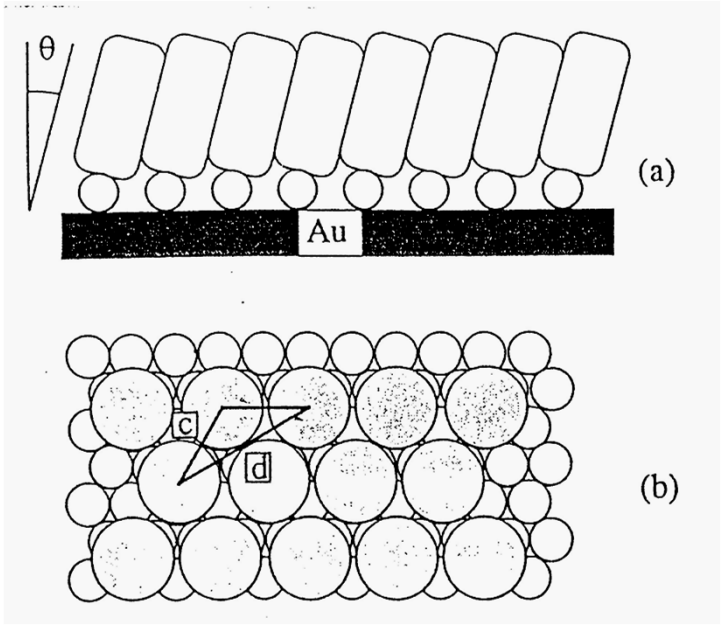

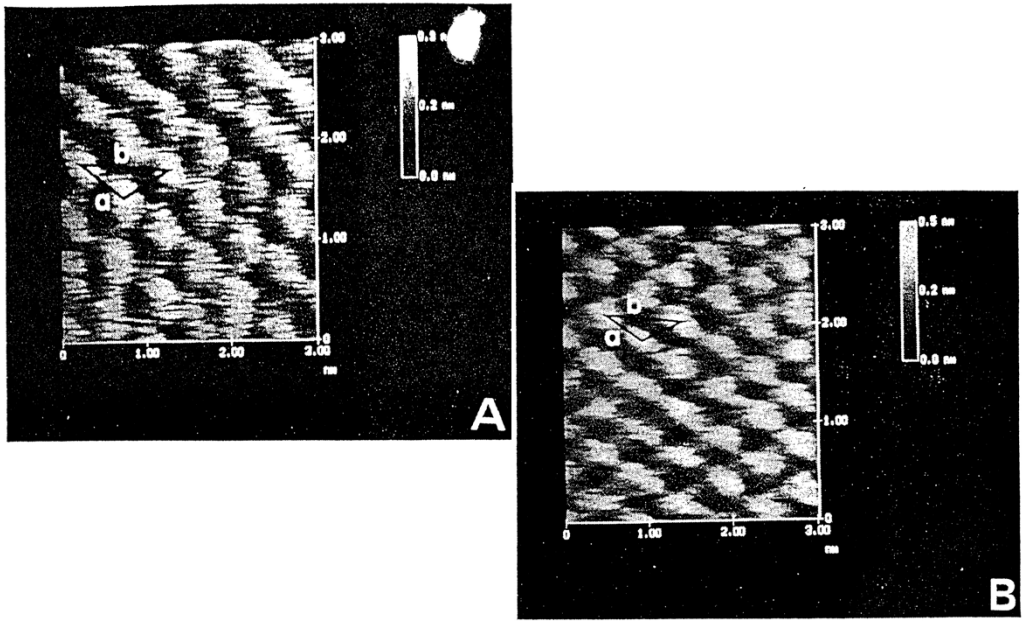

- Schematic illustration of the idealized structure for the monolayer formed from the chemisorption of $CF_3(CF_2)_7(CH_2)2SH$ at Au(111). The tilt(θ) of the perfluorocarbon chains in the side view (A) is 16o with respect to the surface normal. The corresponding (2*2) adlayer structure is depicted in the top view (B). The spacings between adsorbates is 0.58 nm (c) and 1.0 nm (d)

- (A) An AFM image covering 3.0nm*3.0nm of $CF_3(CF_2)_7(CH_2)2SH$ chemisorbed at Au(111). The nearest-neighbor and next-nearest-neighbor spacings are 0.58±0.02 and 1.01±0.02 nm, respectively, as denoted by the lines a and b on the image. This image is unfiltered. (B) An AFM image covering 3.0nm*3.0 nm of decanethiolate at Au(111). The nearest-neighbor and next-nearest-neighbor spacings are 0.50±0.02 and 0.91±0.04 nm, respectively. This image was low pass filtered.

C.A. Alves, E.L Smith, M. D. Porter, *J. Am. Chem. Soc*. 1992, V. 114 (4) P. 1224

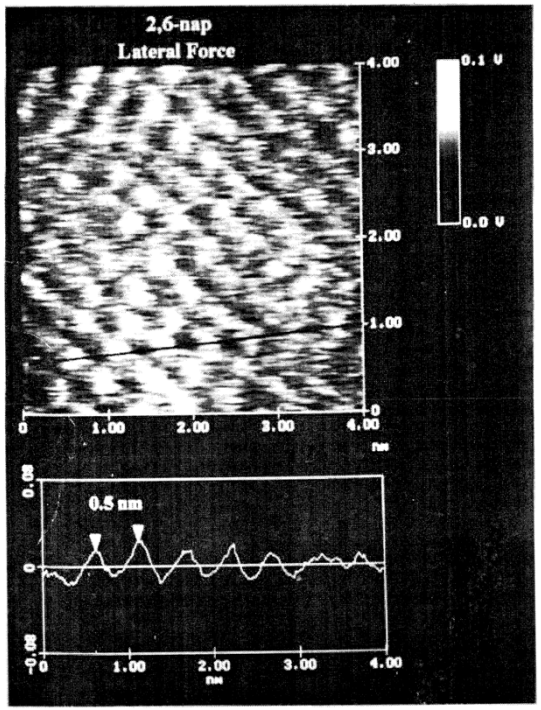

Figure 23.

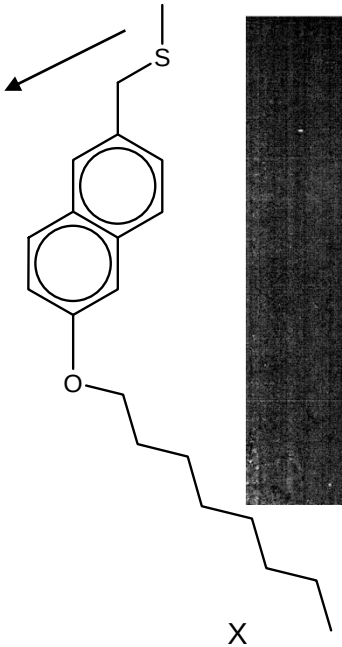

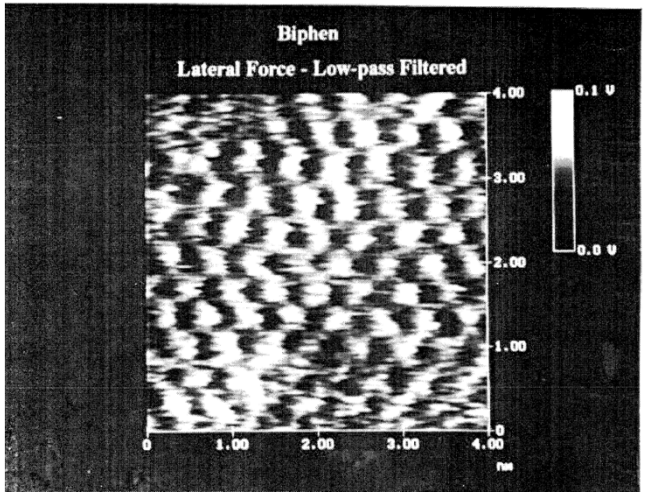

Figure 23.1

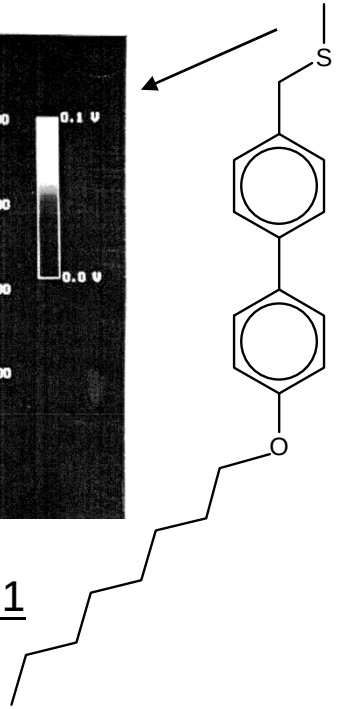

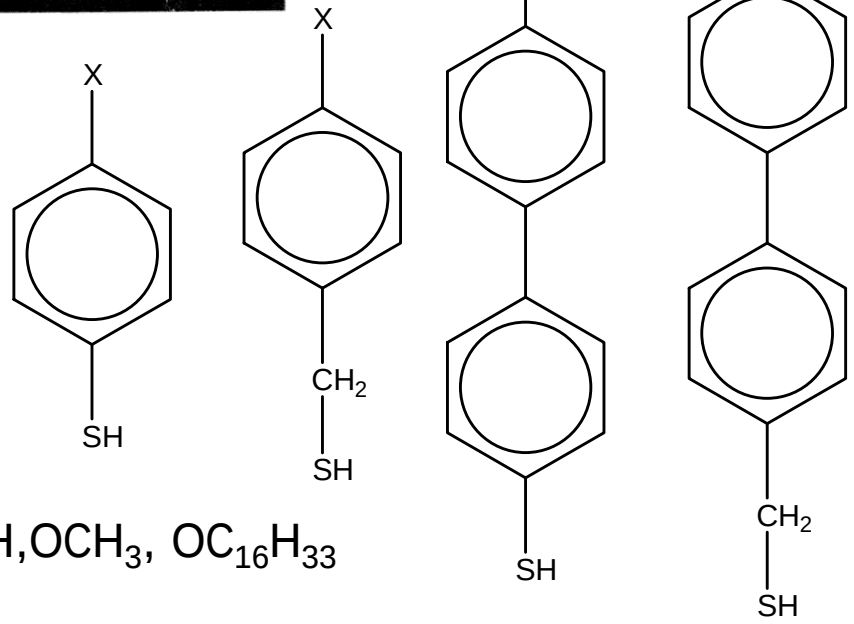

X=H,OCH_3, $OC_{16}H_{33}$

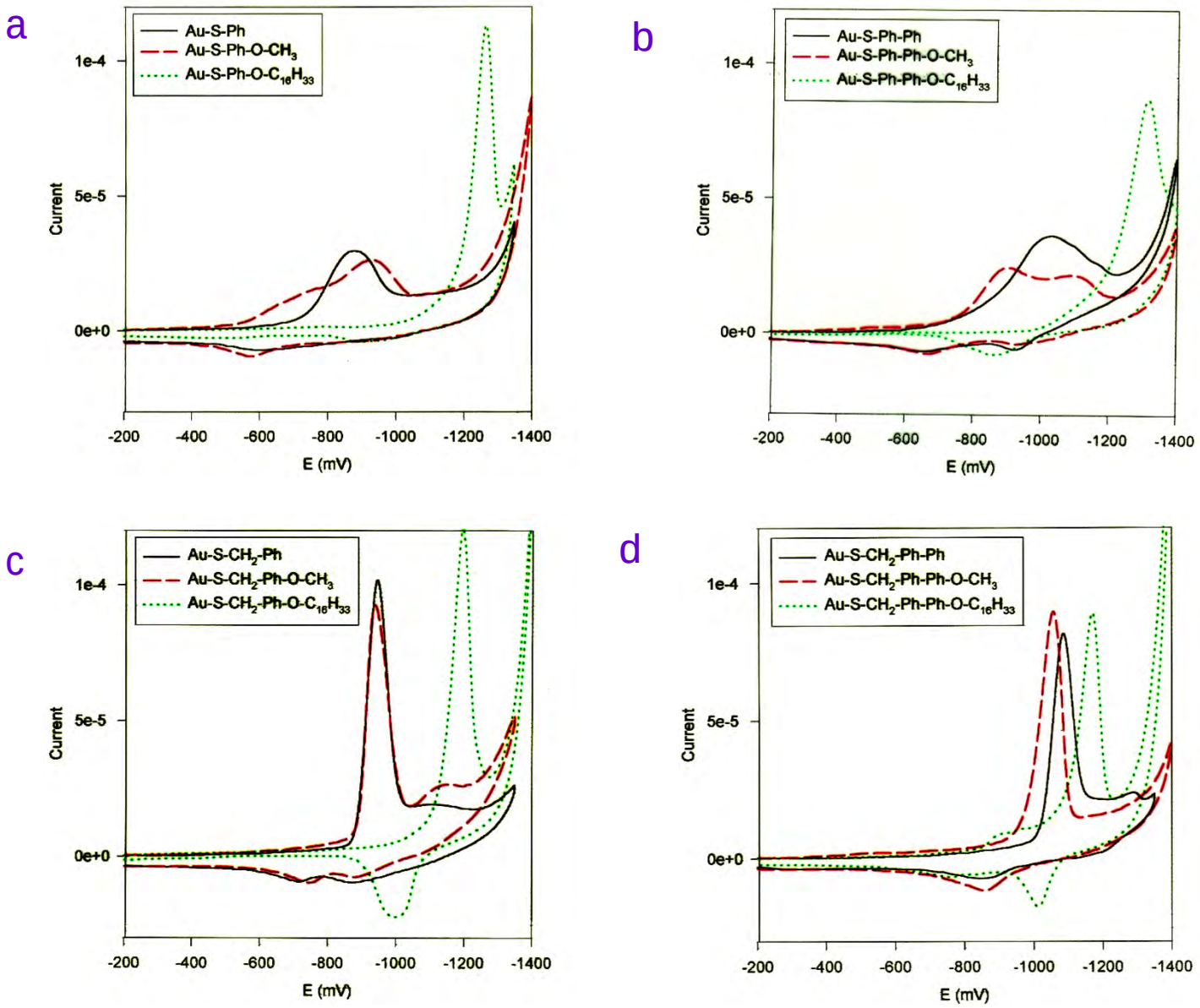
a
Au-S-Ph
Au-S-Ph-O-CH3
Au-S-Ph-O-C16H33
1e-4
5e-5
0e+0
Current
-200
-400
-600
-800
-1000
-1200
-1400
E (mV)
b
Au-S-Ph-Ph
Au-S-Ph-Ph-O-CH3
Au-S-Ph-Ph-O-C16H33
1e-4
5e-5
0e+0
Current
-200
-400
-600
-800
-1000
-1200
-1400
E (mV)
c
Au-S-CH2-Ph
Au-S-CH2-Ph-O-CH3
Au-S-CH2-Ph-O-C16H33
1e-4
5e-5
0e+0
Current
-200
-400
-600
-800
-1000
-1200
-1400
E (mV)
d
Au-S-CH2-Ph-Ph
Au-S-CH2-Ph-Ph-O-CH3
Au-S-CH2-Ph-Ph-O-C16H33
1e-4
5e-5
0e+0
Current
-200
-400
-600
-800
-1000
-1200
-1400
E (mV)

- The packing density (x10-10mol/cm^2) and the desorption potential (mV) in parenthesis of aromatic-derivatized thiols on evaporated Au using electro-chemically reductive desorption method.

X=	I	II	III	IV
H	4.4+0.4(-848)	8.1+0.3(-921)	6.1+0.7(-926)	8.0+0.3(-1091)
OCH_3	5.1+0.3(-921)	8.1+0.3(-939)	5.2+0.8(-907)	8.0+0.1(-1087)
$OC_{16}H_{33}$	6.3+0.6(-1215)	8.0+0.4(-1182)	7.8+0.3(-1305)	7.5+0.3(-1197)
Au-S-$C_{16}H_{33}$	7.8+0.1(-1130)			

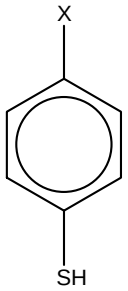

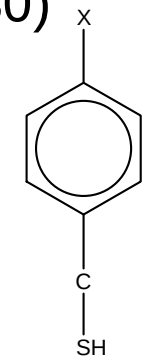

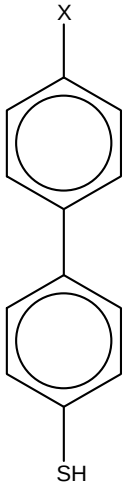

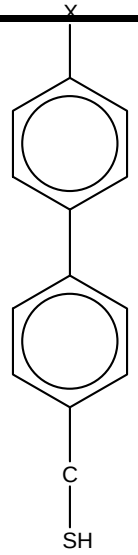

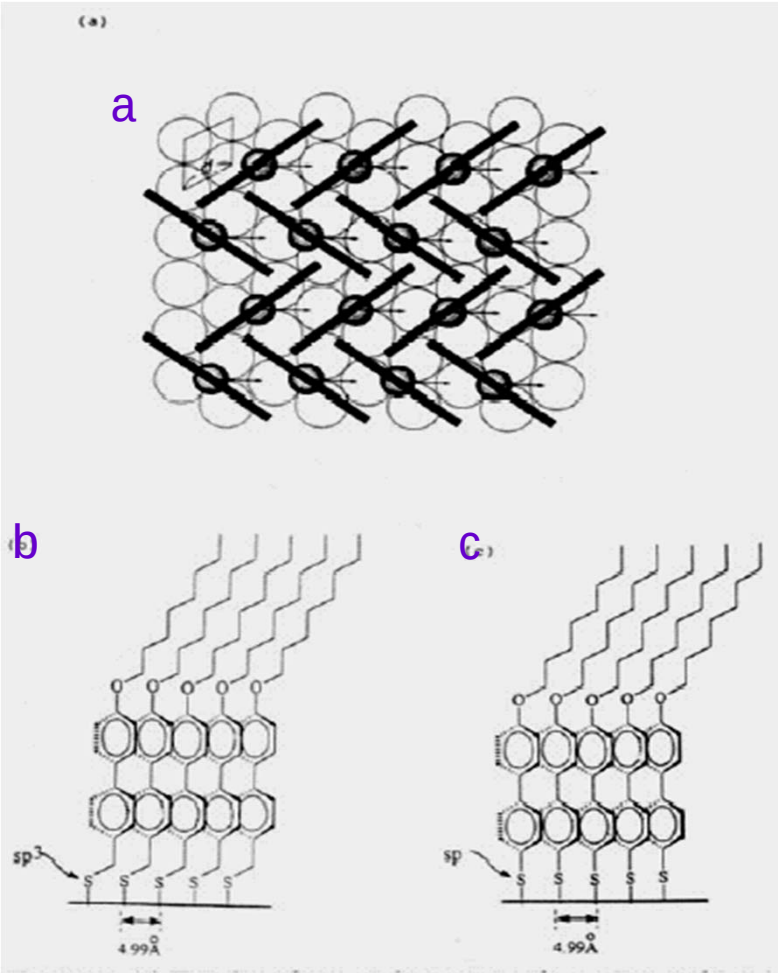

(a) Top view of proposed structures of monolayers of I and III on the (√3*√3) R30° overlayers of Au(111) and Ag(111) surfaces. The arrow indicates the tilting direction of alkyl chain. (b) Side view of monolayer of I along a line connecting the nearest neighbors. (c) Side view of monolayer of III.

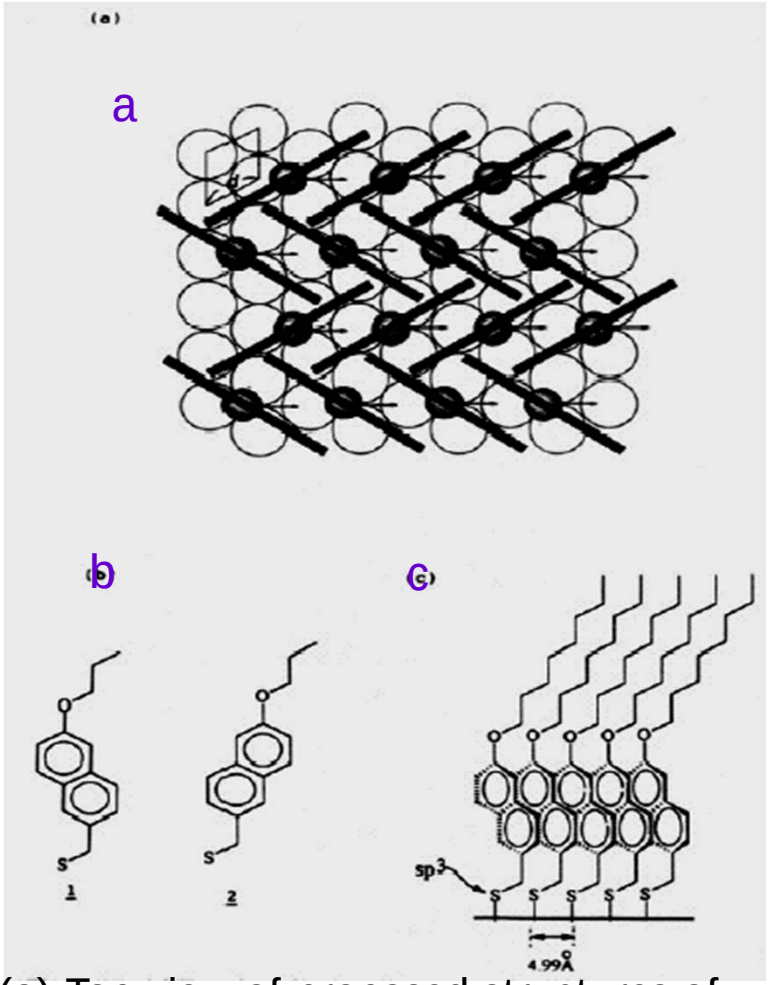

(a) Top view of proposed structures of monolayers of II on the (√3*√3)R30° overlayers of Au(111) and Ag(111) surfaces. The arrow indicates the tilting direction of alkyl chain. (b) Four confirmations for head group. (c) Side view of monolayer along a line connecting the nearest neighbors.

H_2S Induced Reorganization of Self-Assembled Monolayer of n-Alkanethiol Derivatives

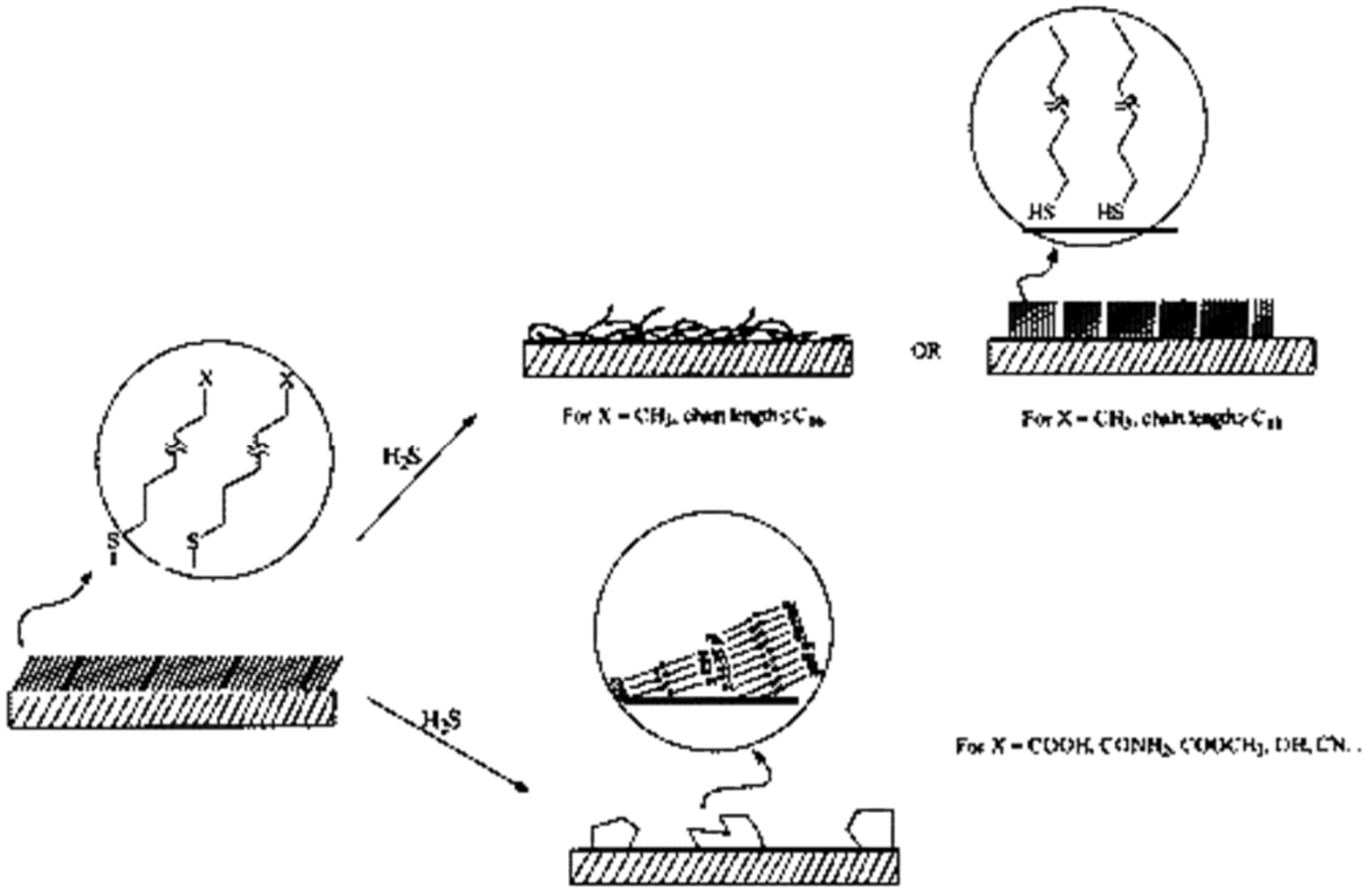

Tao, et al., *J. Am. Chem. Soc.*, 122, 7072 (2000)

Mixed Monolayer System

By coadsorption

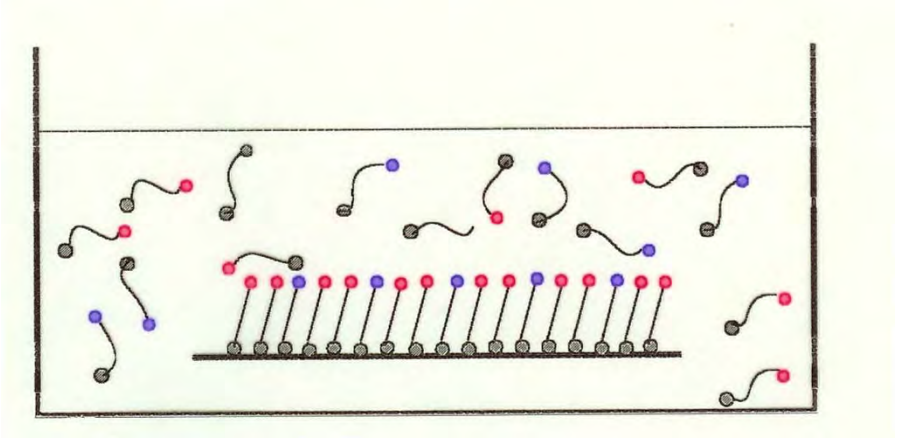

Figure 27. Adsorption from a mixture of components 1 and 2.

By exchange

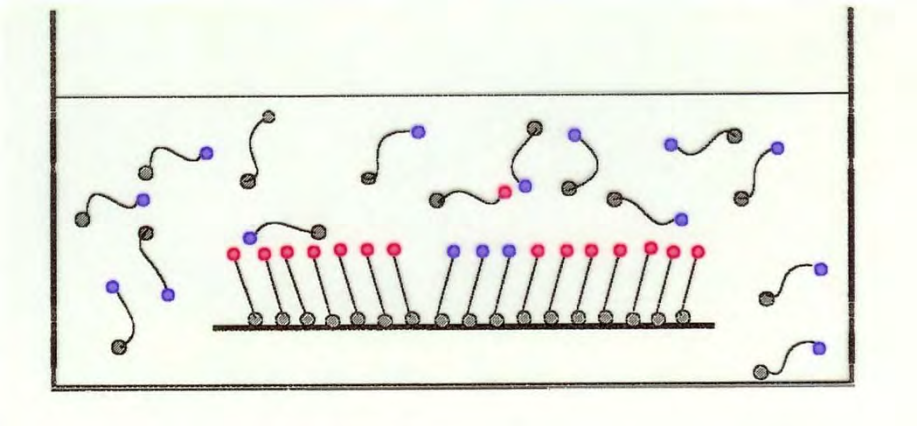

Figure 27.1 A preformed monolayer of component 1 dipped in a solution of component 2.

Structure of Mixed Monolayer

Type A: Two components with same chain length

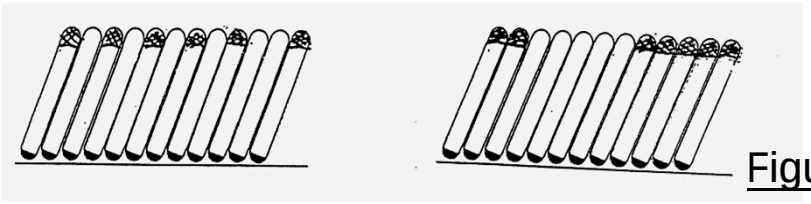

Figure 28.

Type B: Two components with different chain length

(1) Longer polar component

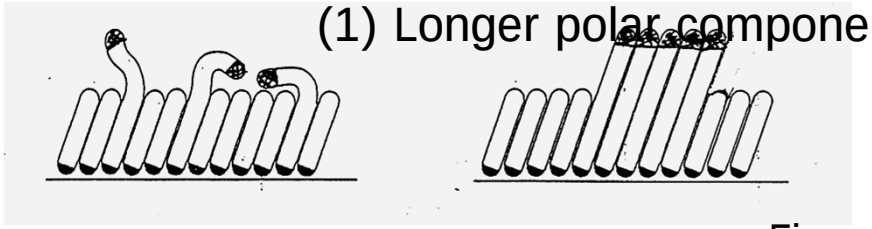

Figure 28.1

(2) Shorter polar component

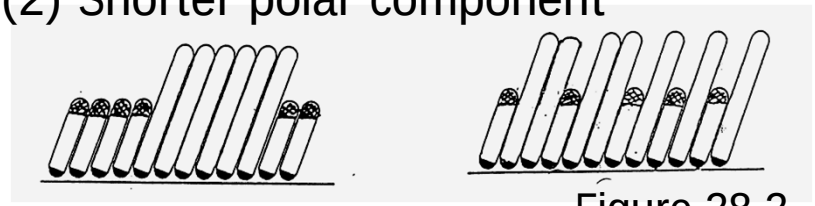

Figure 28.2

Mixed monolayer of p-terphenylcarboxylic acid and hexadecanoic acid

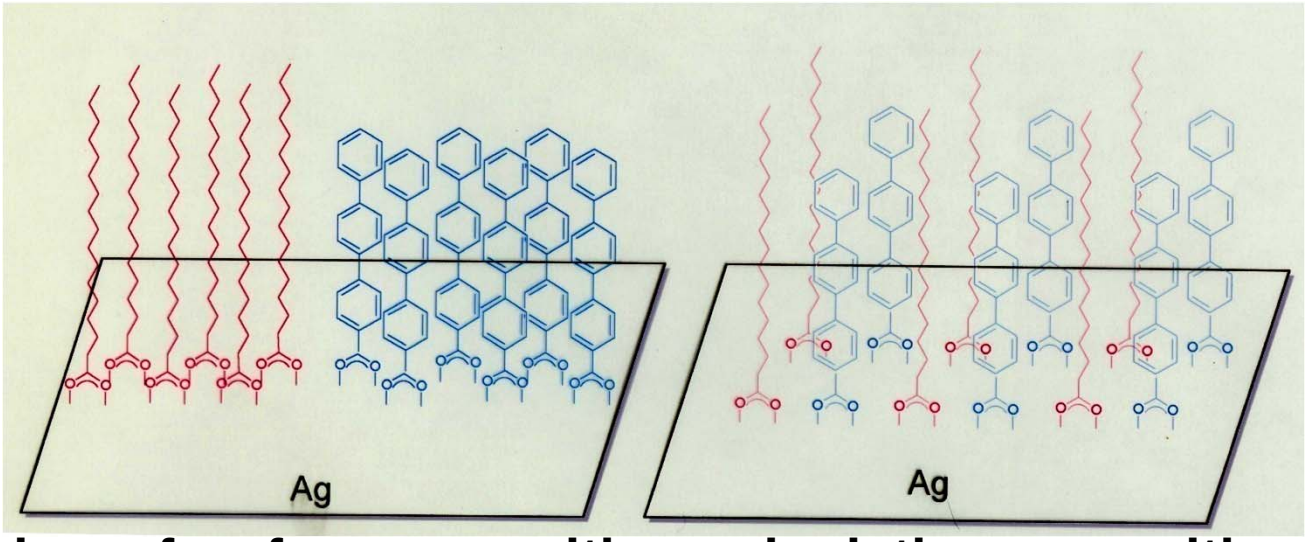

Figure 29.

Comparison of surface composition and solution composition for mixed layer formation of p-terphenylcarboxylic acid and hexadecanoic acid.

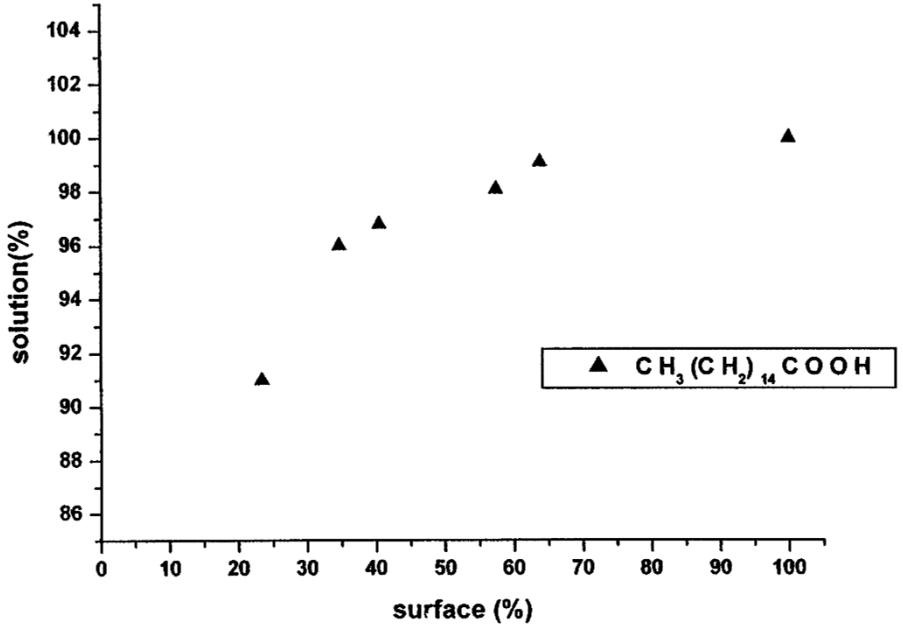

IRS Spectra of Mixed Monolayer of p-terphenylcarboxylic acid and hexadecanoic acid

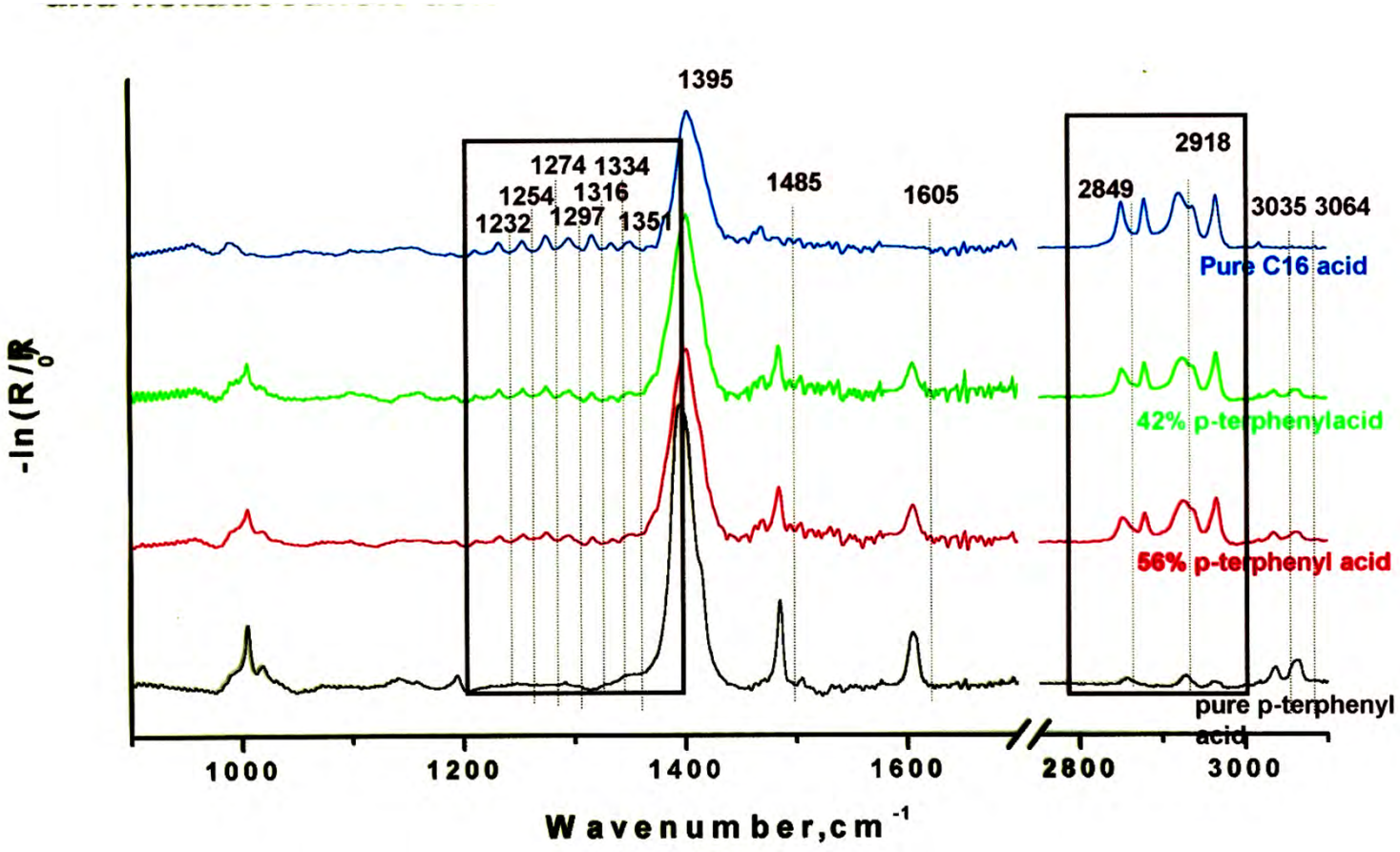

IRS Spectra of H_2S-exposed Mixed Monolayer of p-terphenylcarboxylic acid and *n*-hexadecanoic acid

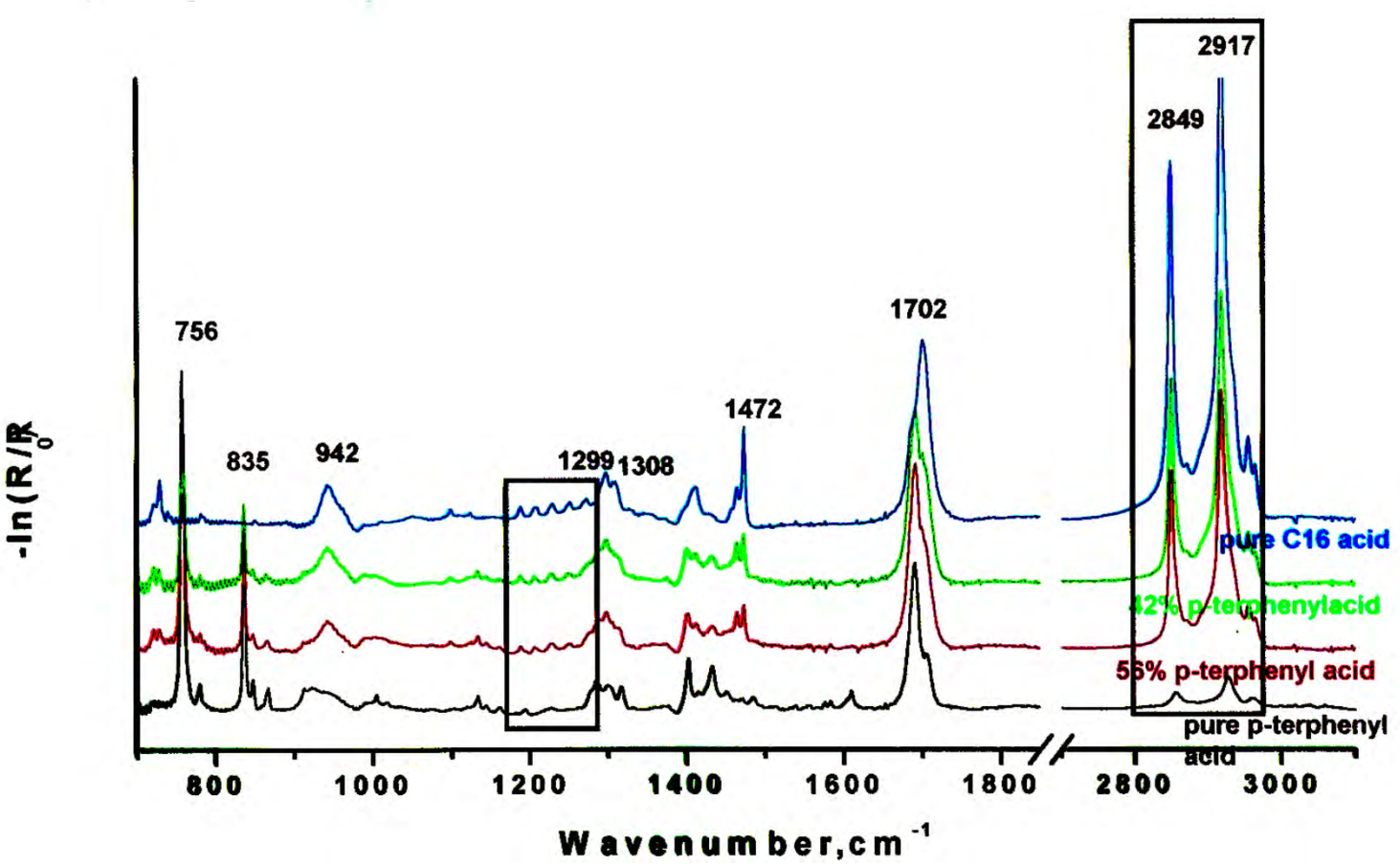

Figure 30.

$CH_3(CH_2)_{15}SH/CH_3OCO(CH_2)_{15}SH$ Mixed SAMs

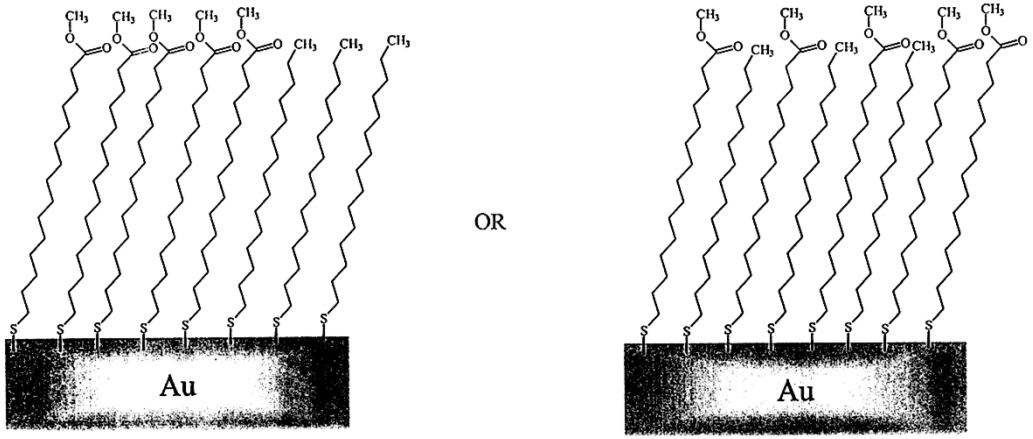

$HS(CH_2)_{15}CH_3/HS(CH_2)_{15}COOCH_3$ Coadsorption

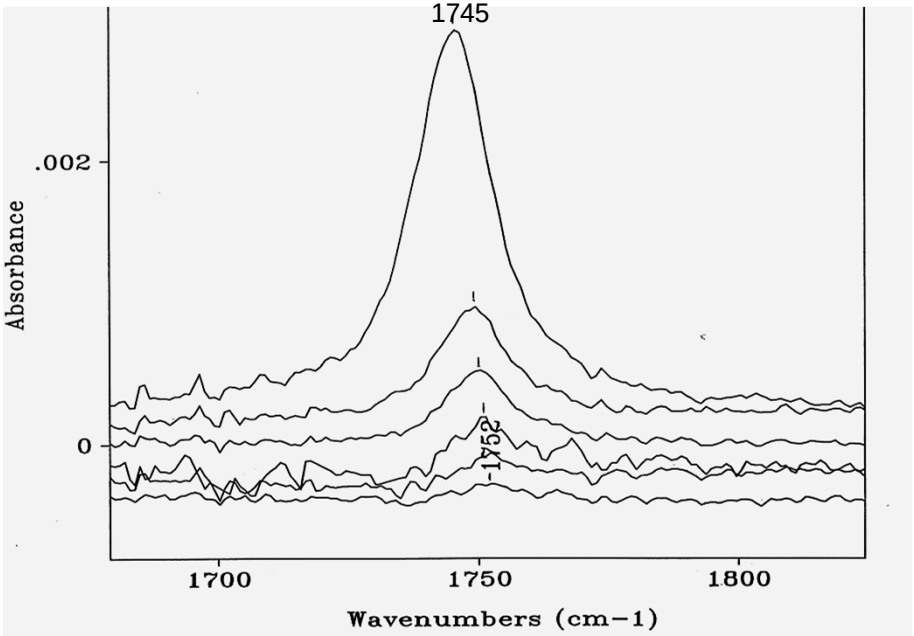

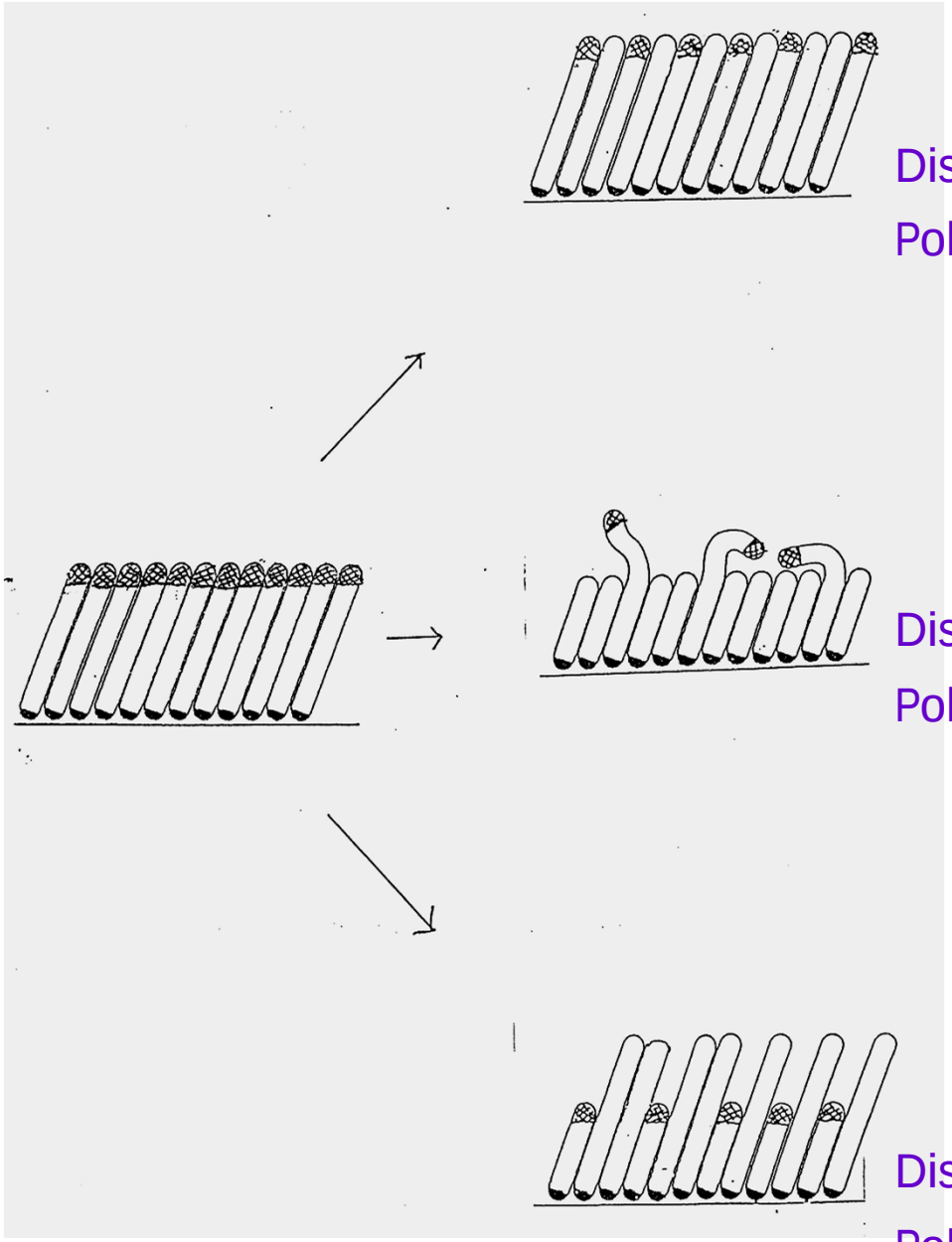

Dispersive interaction

Polar interaction

Dispersive interaction

Polar interaction

Dispersive interaction

Polar interaction

(Left) A scanning tunneling microscope image showing a 500*390 $Å^2$ area of a self-assembled monolayer of a mixture of 20% $CH_3(CH_2)_{15}SH$ and 75% $CH_3O_2C(CH_2)_{15}SH$ on Au. Note the molecular void defect (blue) in the $CH_3(CH_2)_{15}SH$ domain in the lower right area of the image.

(Right) A schematic of the image shown in the left. The domains attributed to the methyl-terminated thiolate are outlined and labeled by M. The region containing a molecular void defect is labeled M'. The single methyl-terminated molecule domains are enclosed in squares.

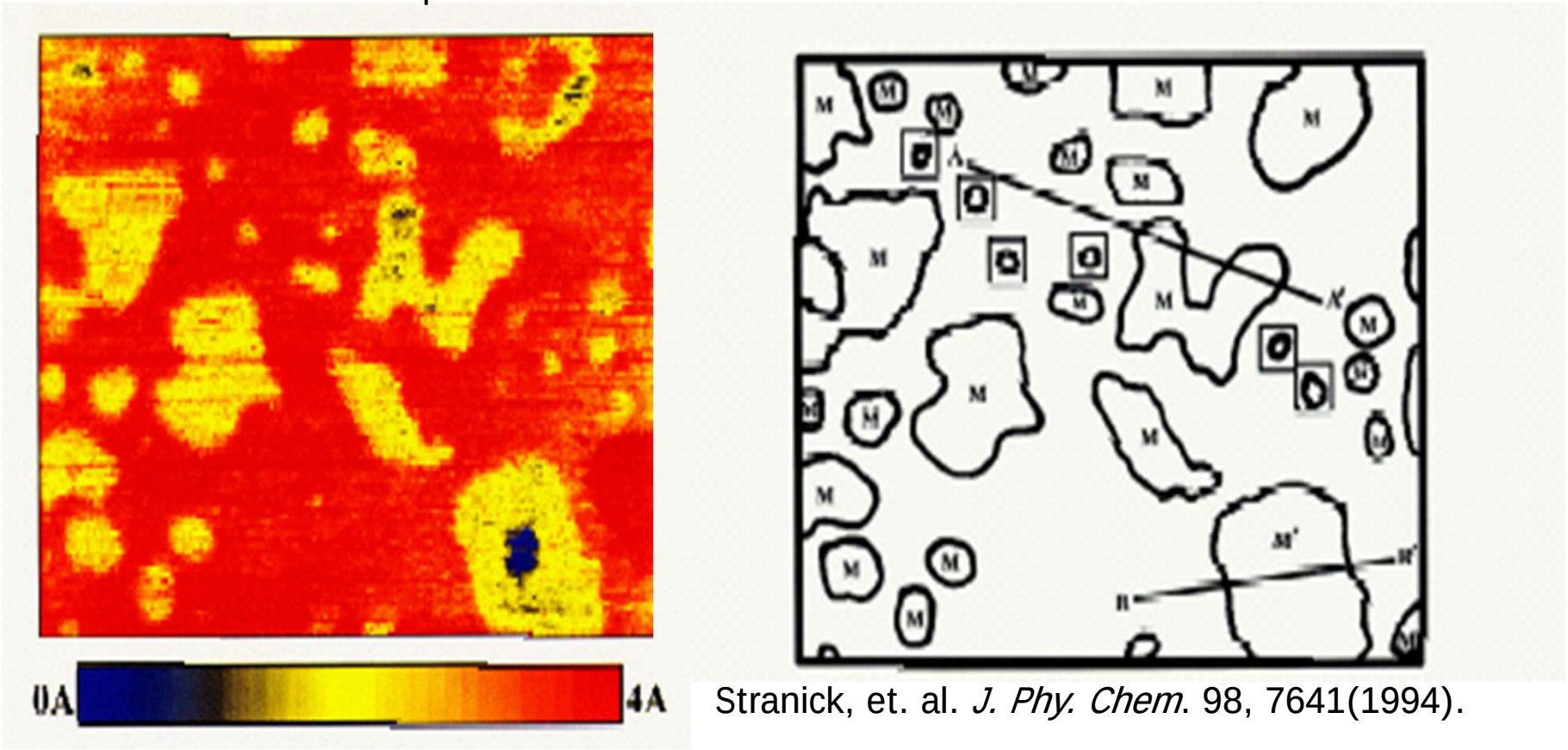

Stranick, et. al. *J. Phy. Chem*. 98, 7641(1994).

Two sequential scanning tunneling microscope images showing a 500*310 $Å^2$ area of a self-assembled monolayer os a mixture of 25% $CH_3(CH_2)_{15}SH$ and 75% $CH_3O_2C(CH_2)_{15}SH$ on Au. The color scale and tunneling conditions are the same as in previous slide. The right image was recorded 37 min. after the left image. Two arrows indicate regions where methyl- and methyl ester-terminated thiolate molecules have exchanged, leading to coalescence of domain of methyl-terminated thiolate molecules.

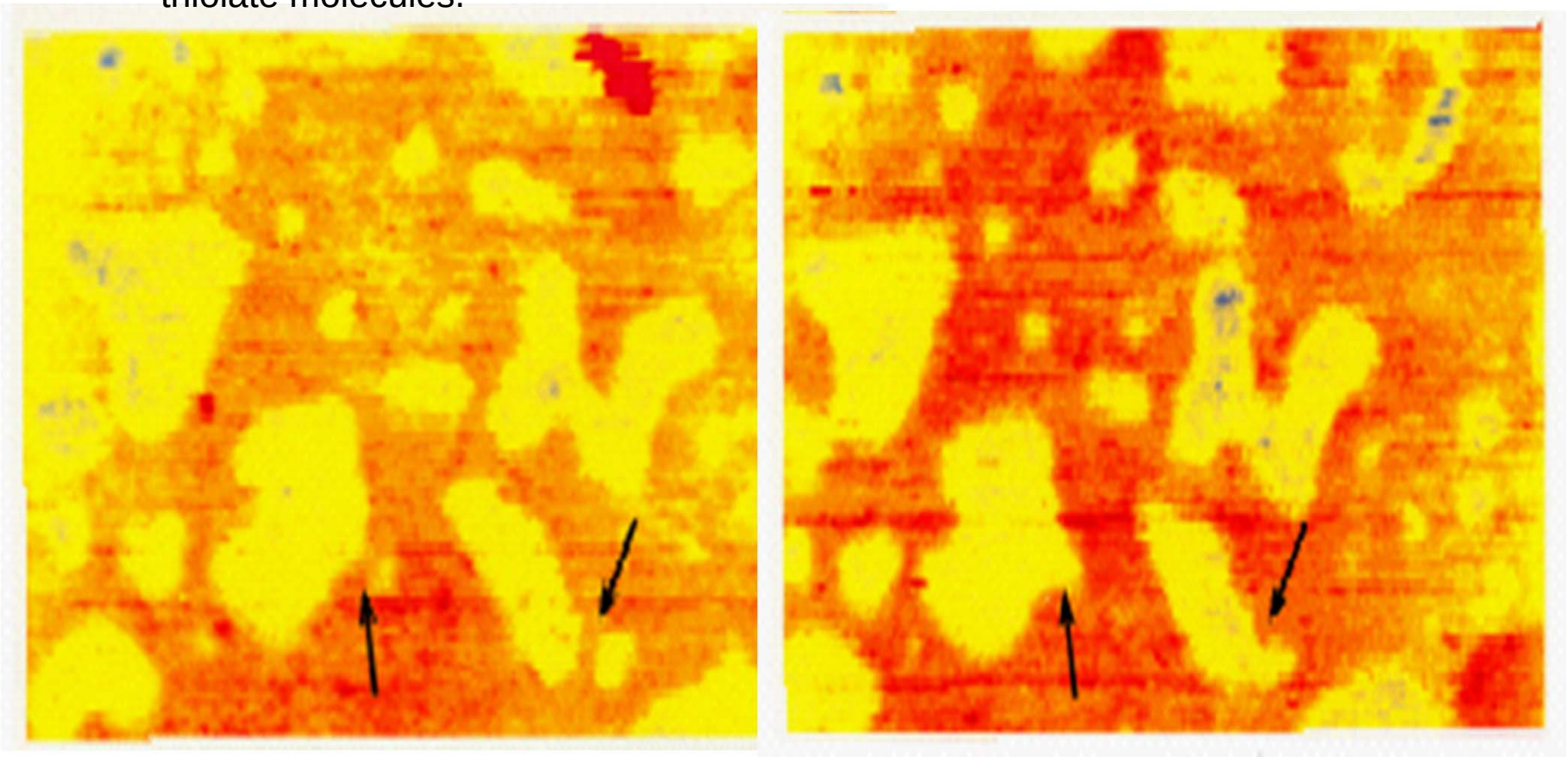

$HO(CH_2)_{16}SH/CH_3OCO(CH_2)_{15}SH$ MIXED SAMs

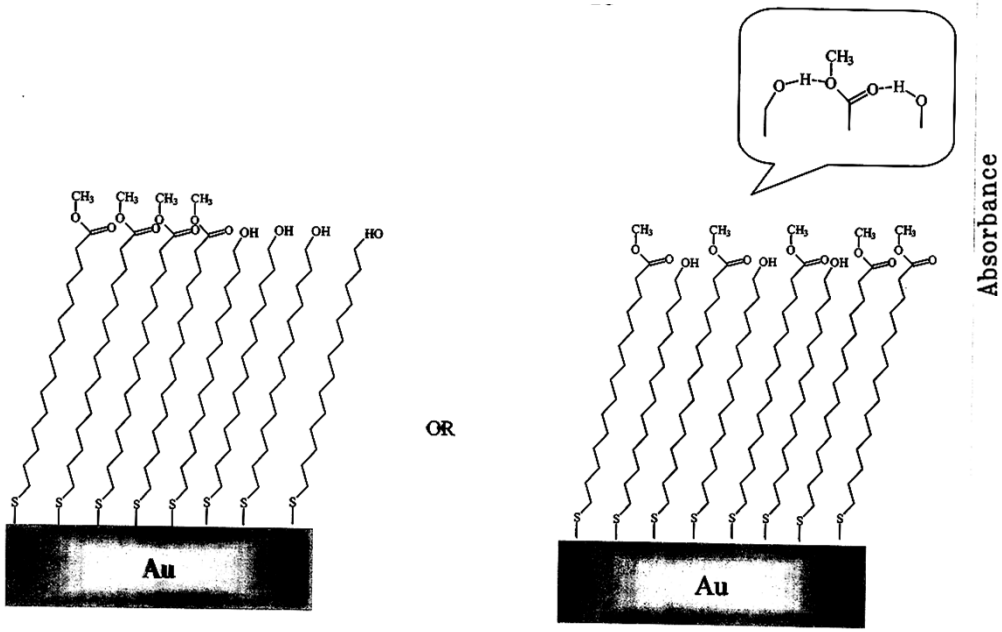

Methyl n-butyrate in Different Phases

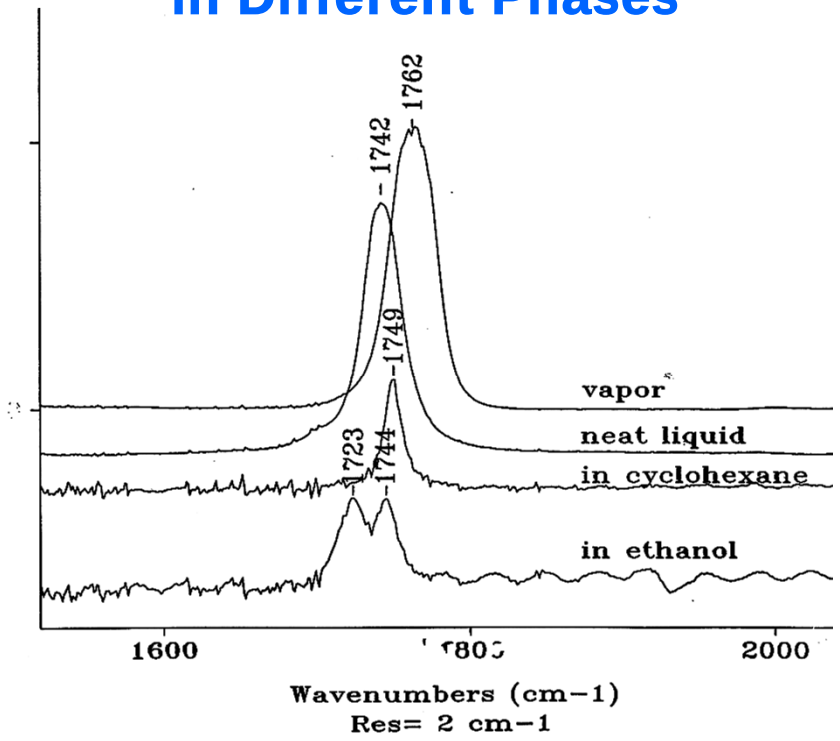

$HS(CH_2)_{16}H/HS(CH_2)_{15}COOCH_3$ Mixed Monolayer

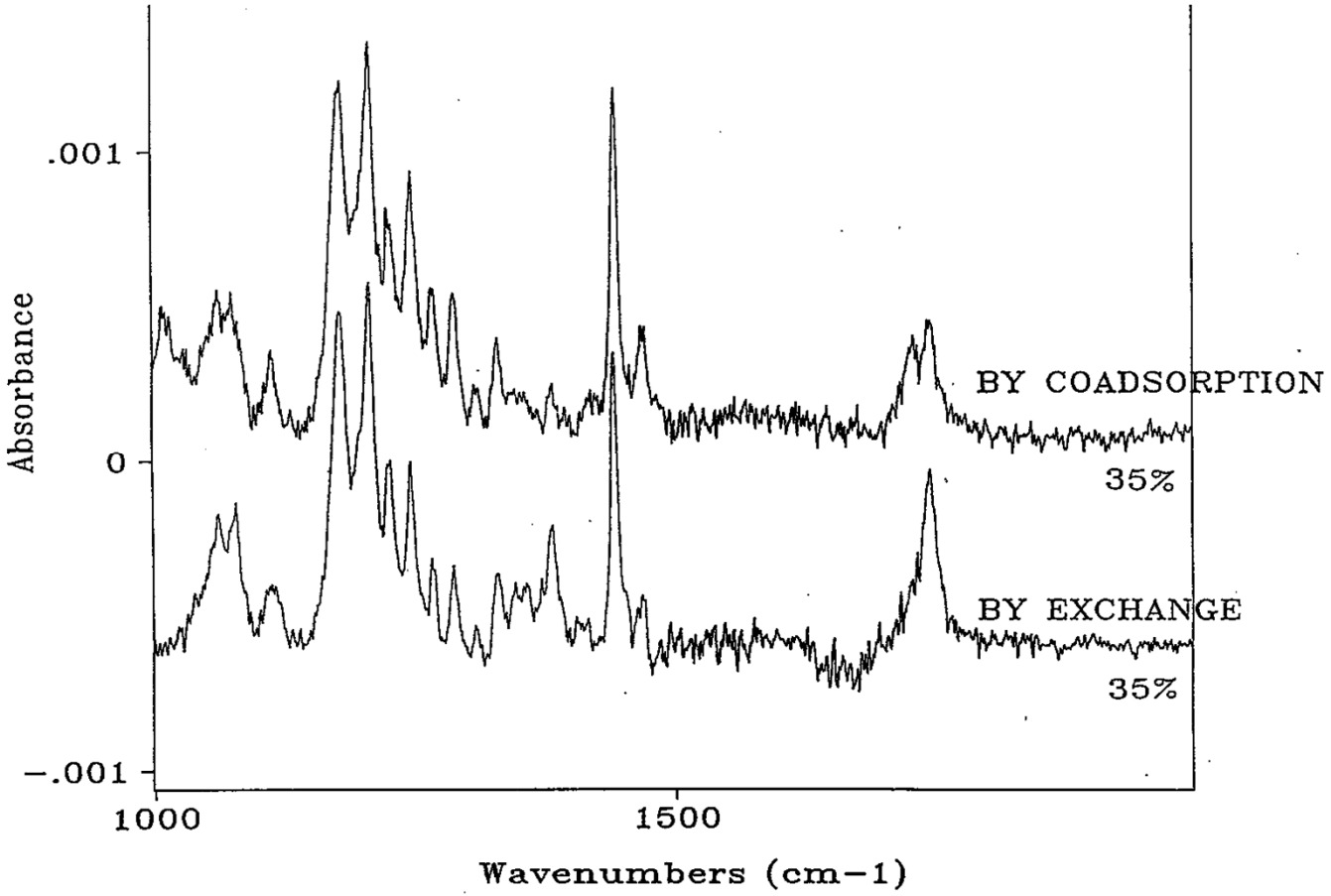

Restoration of Monolayer of p-terphenylcarboxylic acid/hexadecanoic acid at 33°C

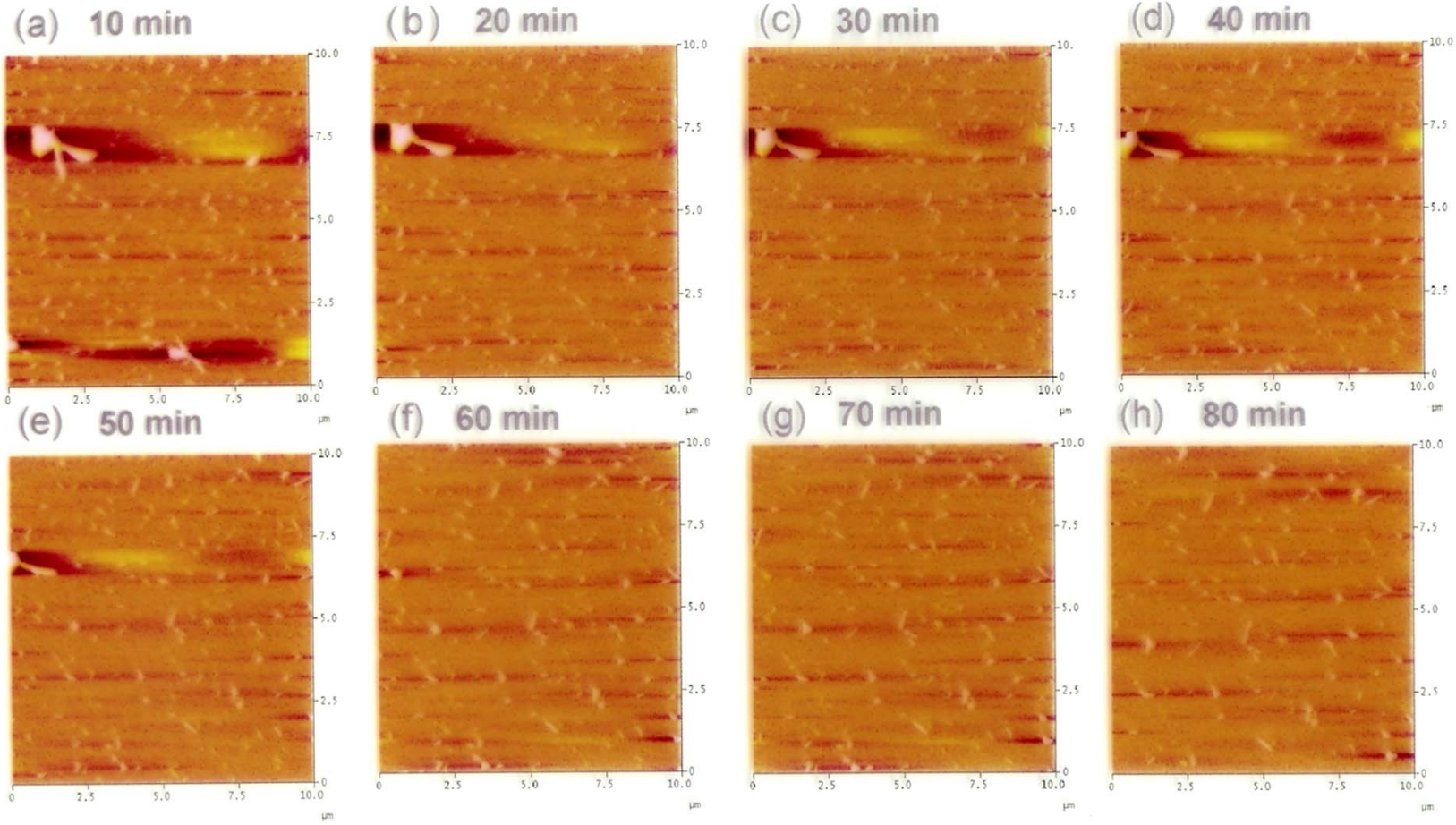

$HC{\equiv}C(CH_2)_{14}SH/C_{12}H_{25}SH$

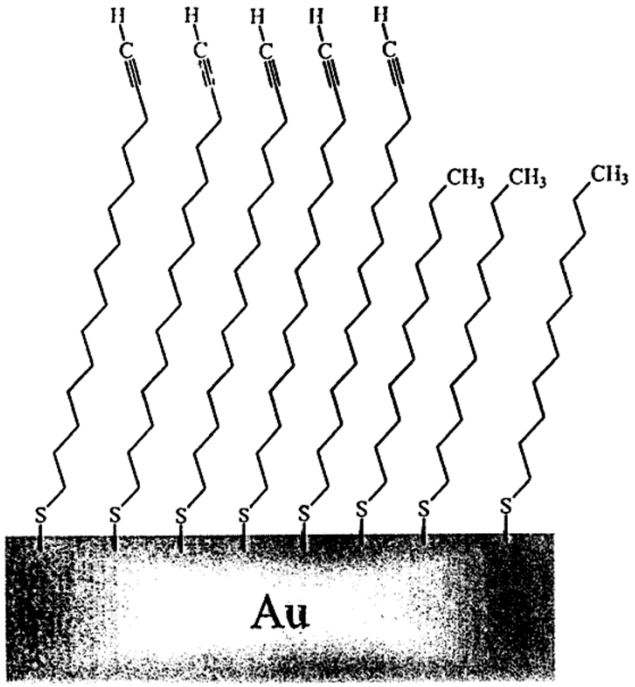

OR

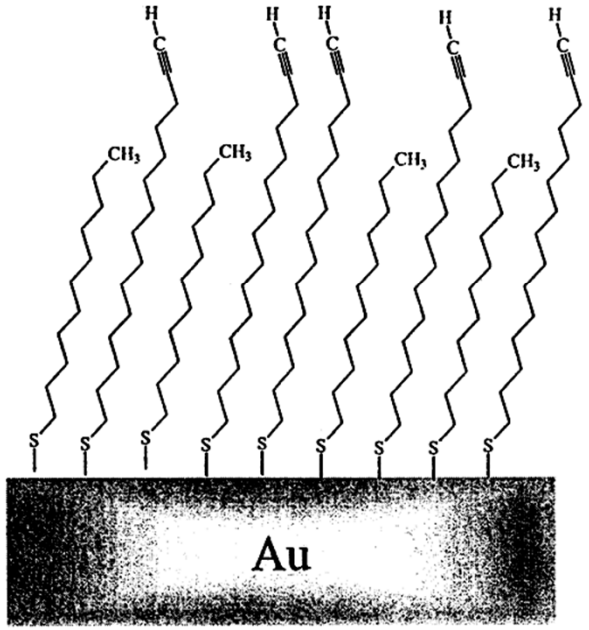

Alkyl Monolayer on Silicon Surface (Chidsey, 1993)

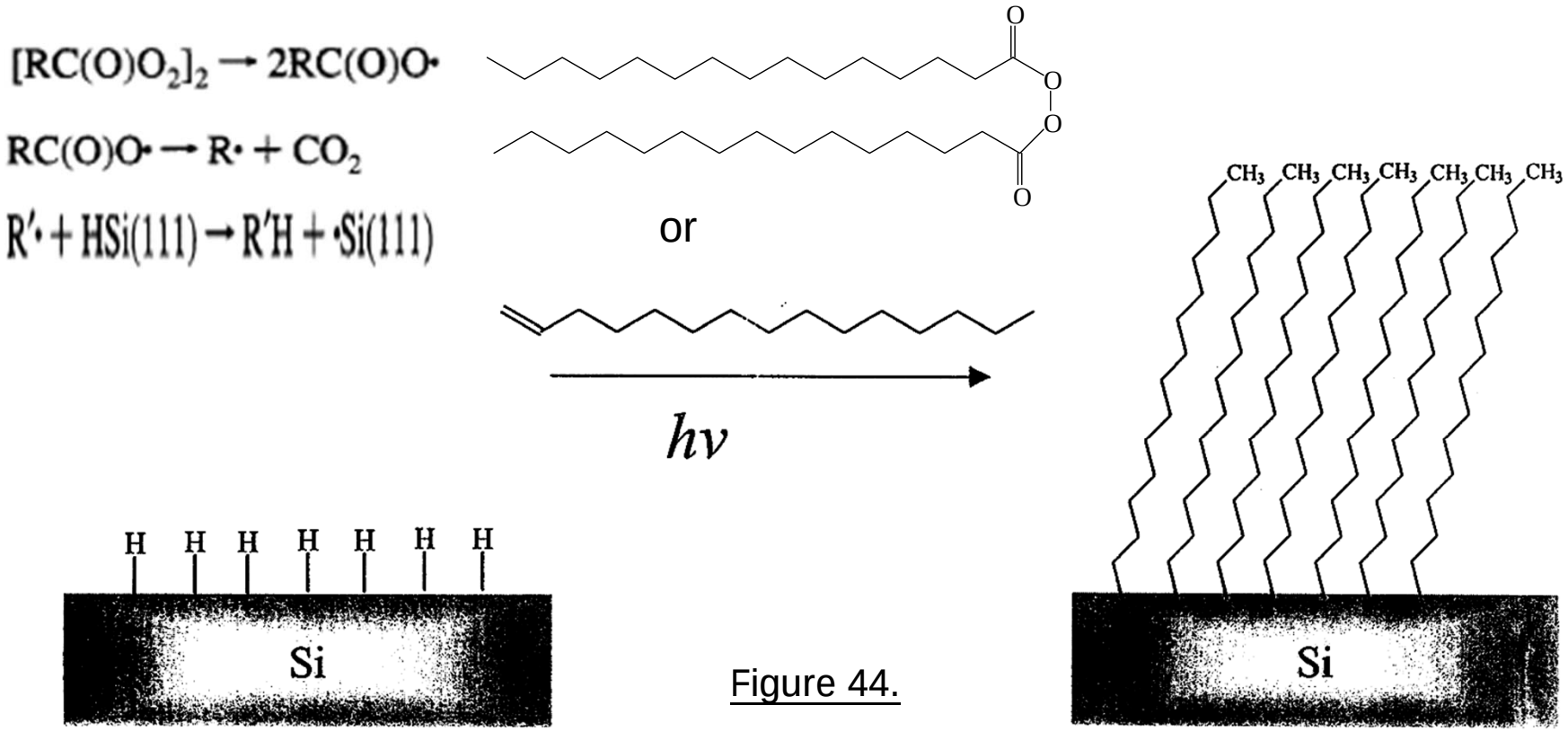

Figure 44.

Stable to boiling H_2O, chloroform, acidic, basic solution,

Multilayer Formation with Polar Order

Sagiv's Approach

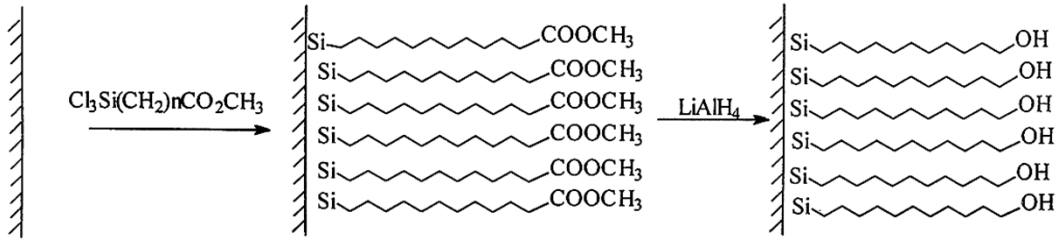

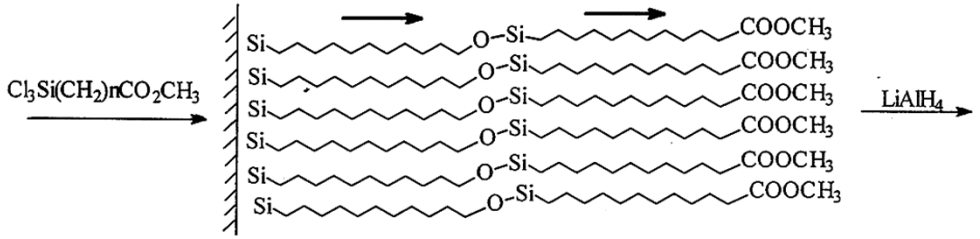

Mallouk's Approach

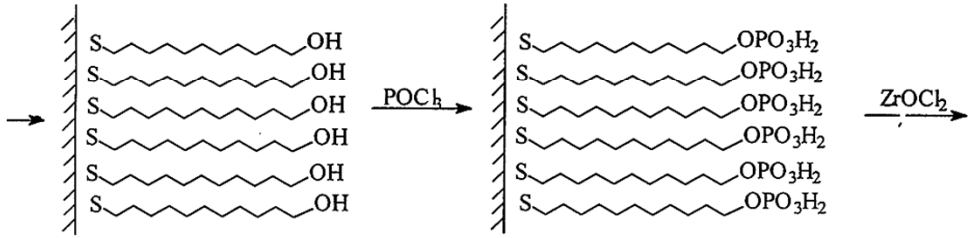

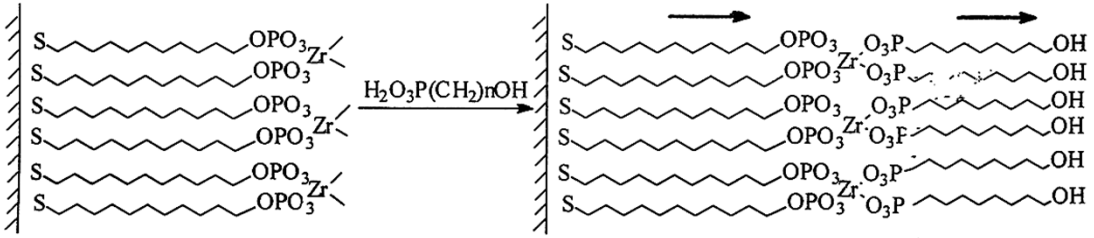

Multilayer Build-up by Self-assembly

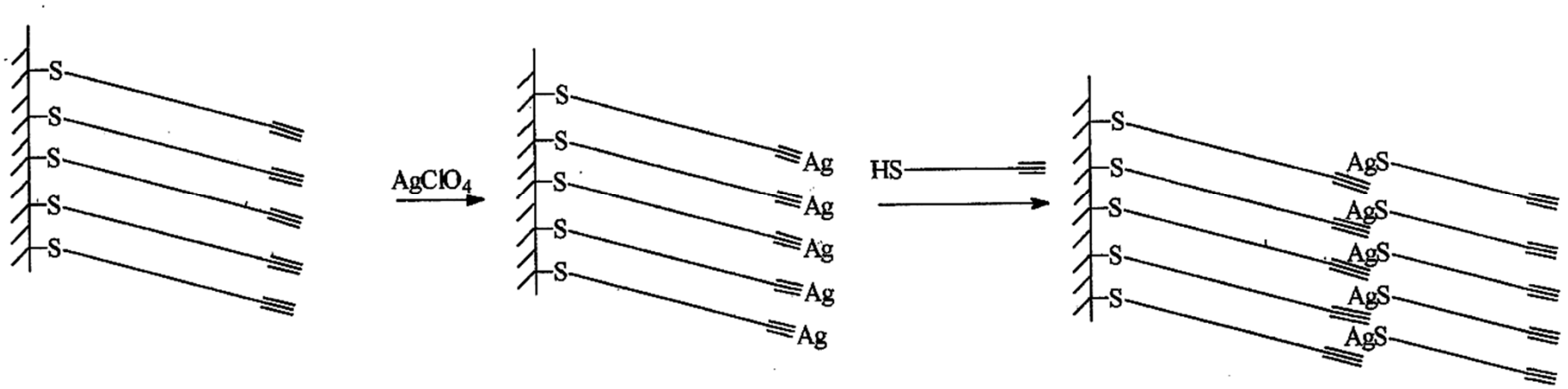

Figure 44.

Monolayer Protected Clusters (MPC)

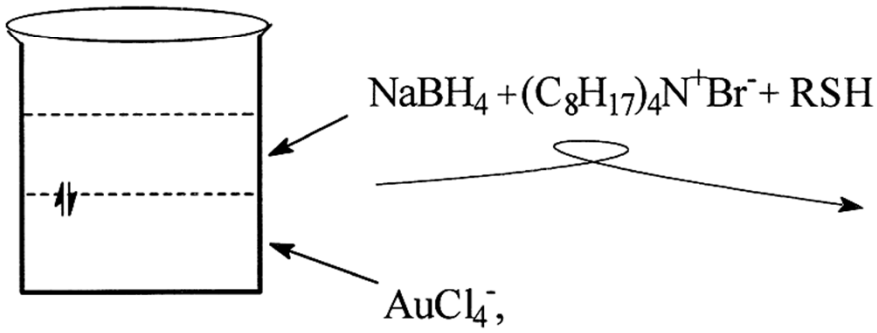

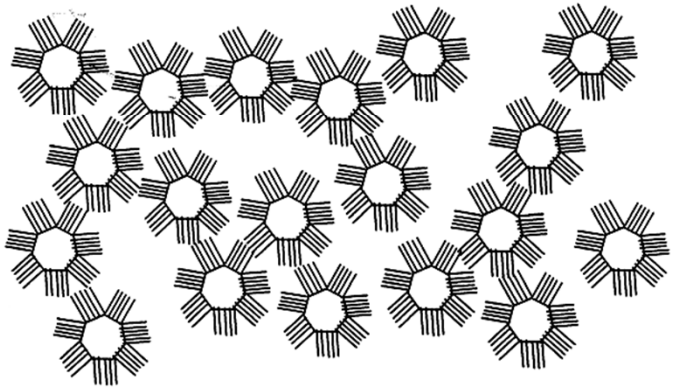

$$AuCl_4^-(\text{toluene}) + RSH \longrightarrow (-Au^{I}SR-)_n(\text{polymer})$$

$$(-Au^{I}SR-)_n + BH_4^- \longrightarrow Au_x(SR)_y$$

M. Brust, et al *J. Chem. Soc. Chem. Commun.* **1994**, 801.

The surface functional group can be replaced by another functional thiol.

Characteristics of the Nucleation-Growth-Passivation Process:

1. Larger thiol: gold mole ratios give smaller average MPC core sizes.
2. Fast reduction and cooled solutions produce smaller, more monodispersed MPCs.
3. Quenching the reaction immediately following the reduction produces smaller core sizes.

- Core Metals: Au, Ag, Au/Ag, Au/Cu, Au/Ag/Cu, Au/Pt, Au/Pd, Au/Ag/Cu/Pd
- Ligands: Alkanethiols, disulfides, ω-functionalized thiols, arenethiols…

Reactivity of Monolayer-Protected Clusters

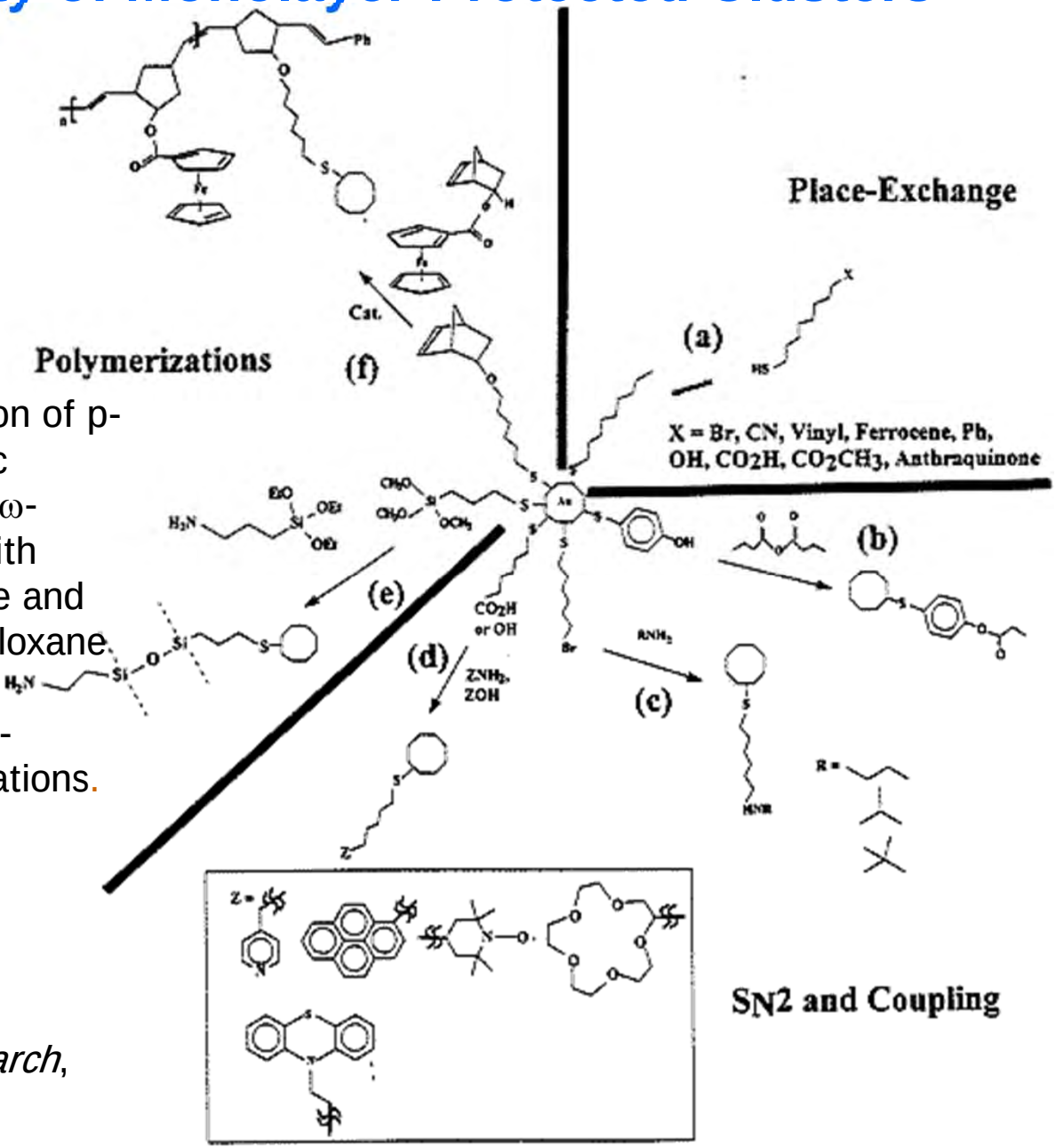

(a) Place-exchange. (b) reaction of p-mercaptophenol with propionic anhydride. (c) S_N2 reaction of ω-bromoalkanethiolated MPCs with primary alkylamines. (d) amide and ester coupling reactions. (e) siloxane formation reactions. And (f) transition-metal-catalyzed ring-opening metathesis polymerizations.

Account of Chemistry Research, V. 33 (1) P. 27